Intercomparison of SCIAMACHY nitrogen dioxide observations, in situ measurements and air quality modeling results over Western Europe

N. Blond, K. F Boersma, H. Eskes, R. van Der A, M. van Roozendael, I. de Smedt, G. Bergametti, R. Vautard

JOURNAL OF GEOPHYSICAL RESEARCH, VOL. 112, D10311, doi:10.1029/2006JD007277, 2007

Intercomparison of SCIAMACHY nitrogen dioxide observations, in situ measurements and air quality modeling results over Western Europe

N. Blond,[1] K. F. Boersma,[2] H. J. Eskes,[2] R. J. van der A,[2] M. Van Roozendael,[3] I. De Smedt,[3] G. Bergametti,[1] and R. Vautard[4]

Received 8 March 2006; revised 26 January 2007; accepted 31 January 2007; published 24 May 2007.

[1] The Scanning Imaging Absorption Spectrometer for Atmospheric Cartography (SCIAMACHY) satellite spectrometer provides detailed information on the nitrogen dioxide (NO_2) content in the planetary boundary layer. NO_2 tropospheric column retrievals of SCIAMACHY and its predecessor Global Ozone Monitoring Experiment are characterized by errors of the order of 40%. We present here a new SCIAMACHY tropospheric retrieval data set for the year 2003. The cloud free satellite observations are compared to surface measurements and simulations over western Europe performed with the regional air-quality model CHIMERE. The model has a resolution of 50 km similar to the satellite observations. For these comparisons, averaging kernels are applied to the collocated model profiles to remove the dependency of the comparison on a priori NO_2 profile information used in the retrieval. The consistency of both SCIAMACHY and CHIMERE outputs over sites where surface measurements are available allows us to be confident in evaluation of the model over large areas not covered by surface observations. CHIMERE underestimates surface NO_2 concentrations for urban and suburban stations which we mainly attribute to the low representativeness of point observations. No such bias is found for rural locations. The yearly average SCIAMACHY and CHIMERE spatial NO_2 distributions show a high degree of quantitative agreement over rural and urban sites: a bias of 5% (relative to the retrievals) and a correlation coefficient of 0.87 ($n = 2003$). On a seasonal basis, biases are smaller than 20% and correlation coefficients are larger than 0.75. Spatial correlations between both the model and satellite columns and the European Monitoring and Evaluation Program (EMEP) emission inventory are high in summer ($r = 0.74$, $n = 1779$) and low in winter ($r = 0.48$, $n = 1078$), related to seasonal changes in lifetime and transport. On the other hand, CHIMERE and SCIAMACHY columns are mutually consistent in summer ($r = 0.82$) and in winter ($r = 0.79$). This shows that CHIMERE simulates the transport and chemical processes with a reasonable accuracy. The NO_2 columns show a high daily variability. The daily NO_2 pollution plumes observed by SCIAMACHY are often well described by CHIMERE both in extent and in location. This result demonstrates the capabilities of a satellite instrument such as SCIAMACHY to monitor the NO_2 concentrations over large areas on a daily basis. It provides evidence that present and future satellite missions, in combination with CTM and surface data, will contribute to improve quantitative air quality analyses at a continental scale.

Citation: Blond, N., K. F. Boersma, H. J. Eskes, R. J. van der A, M. Van Roozendael, I. De Smedt, G. Bergametti, and R. Vautard (2007), Intercomparison of SCIAMACHY nitrogen dioxide observations, in situ measurements and air quality modeling results over Western Europe, *J. Geophys. Res.*, *112*, D10311, doi:10.1029/2006JD007277.

1. Introduction

[2] Satellite observations of the tropospheric composition have recently become available. The Global Ozone Monitoring Experiment (GOME) spectrometer on European Space Agency (ESA) ERS-2 [*Burrows et al.*, 1999] has demonstrated its ability to observe columns of trace gases in the troposphere, including the contribution from the boundary layer. Measurements of tropospheric columns of NO_2, formaldehyde (HCHO) [e.g., *Chance et al.*, 2000], sulfur

[1]Laboratoire Interuniversitaire des Systèmes Atmosphériques, UMR CNRS 7583, Universités Paris 7 et 12, Créteil, France.
[2]Atmospheric Composition Climate Research, Royal Netherlands Meteorological Institute, De Bilt, Netherlands.
[3]Belgian Institute for Space Aeronomy, Brussels, Belgium.
[4]Laboratoire de Météorologie Dynamique, UMR CNRS 8539, École Polytechnique, Palaiseau, France.

0148-0227/07/2006JD007277$09.00

dioxide (SO_2) [e.g., *Eisinger and Burrows*, 1998], and ozone (O_3) [e.g., *Valks et al.*, 2003] have been described in recent articles. NO_2 measurements have received considerable attention. Several groups have developed retrieval approaches to derive tropospheric NO_2 columns from GOME [e.g., *Leue et al.*, 2001; *Richter and Burrows*, 2002; *Martin et al.*, 2002; *Boersma et al.*, 2004]. Eight years of NO_2 measurements are now available based on GOME, and this record is extending with Scanning Imaging Absorption Spectrometer for Atmospheric Cartography (SCIAMACHY) aboard ENVISAT [e.g., *Bovensmann et al.*, 1999; *van der A et al.*, 2006] launched in 2002. With a resolution of 30×60 km^2, SCIAMACHY reaches the scale of NO_2 urban plumes for major cities. Such satellite observations, together with infrared satellite observations of tropospheric carbon monoxide [*Emmons et al.*, 2004], ozone, other gaseous species, and measurements of aerosols by dedicated instruments [*Chu et al.*, 2003; *Wang and Christopher*, 2003], offer new perspectives to study air pollution.

[3] In parallel with the development of remote-sensed global observation of tropospheric content, various chemistry transport models (CTMs) have been developed over the last 20 years in order to understand and forecast air pollution. These CTMs cover different spatial scales ranging from continental (for example, for Europe [*Zlateve et al.*, 1992; *Builtjes*, 1992; *Hass et al.*, 1997; *Schmidt et al.*, 2001; *Simpson et al.*, 2003]) to urban (for example, for Los Angeles [*Lu et al.*, 1997a, 1997b]; for Milan [*Silibello et al.*, 1998]; for Atlanta [*Cardelino et al.*, 2001]; for Paris [*Vautard et al.*, 2001]). These models require accurate input data, but most of these (emissions, initial and boundary conditions, meteorology) remain uncertain (several references about uncertainties may be found in the work of *Beekmann and Derognat* [2003]). The model evaluation has always been based on comparison with surface and airborne observations which have limited spatial extent or representativeness, for example, for ozone [*Elbern and Schmidt*, 2001; *Tilmes et al.*, 2002; *Blond and Vautard*, 2004] and for other species including NO_2 and aerosols [*Schmidt et al.*, 2001; *Hodzic et al.*, 2005]. Model performance evaluation in the free troposphere is hampered by the lack of routine data above the surface. Because long-range transport of pollutants is linked to vertical exchange between the boundary layer and the free troposphere, testing the capability of the models to simulate vertical distribution of pollutants is a key issue to evaluate their performance. In this way, satellite observations offer new opportunities to model evaluation and to improve the capabilities of these models.

[4] However, space-borne tropospheric trace gas retrievals, and NO_2 tropospheric column retrievals in particular, are subject to several sources of uncertainty because of the presence of clouds, the accuracy of albedo maps, the dependence on the a priori assumed NO_2 profile, and the presence of aerosols [*Boersma et al.*, 2004]. The retrieval of tropospheric NO_2 columns from GOME and SCIAMACHY satellite measurements remains largely invalidated because of limited availability of independent measurements. For the GOME tropospheric NO_2 columns, only a few intercomparisons with aircraft and in situ measurements have been reported [e.g., *Heland et al.*, 2002; *Petritoli et al.*, 2004; *Martin et al.*, 2004; *Schaub et al.*, 2006]. Unfortunately only a limited number of measured profiles are available for such intercomparisons, and the representativeness of the results is thus a complicating issue, given the large variability of nitrogen oxides ($NO_x = NO + NO_2$) in industrialized regions and the large footprint of the satellite measurements.

[5] The GOME-derived tropospheric NO_2 columns have been compared to several global-scale atmospheric models [e.g., *Velders et al.*, 2001; *Lauer et al.*, 2002; *Savage et al.*, 2004]. Recently, monthly means of GOME-derived tropospheric NO_2 columns have been compared to the outputs of the high-resolution regional-scale CTM model CHIMERE during one summer season [*Konovalov et al.*, 2004]. These comparisons have clearly demonstrated the potential of satellite NO_2 data sets for model validation. However, the monthly mean comparisons do not allow to examine the large day-to-day variability due to meteorological conditions. A collocation in both space and time (as opposed to a comparison of monthly mean values) is essential to obtain quantitative results.

[6] The validation of early SCIAMACHY NO_2 products is described by *Lambert et al.* [2004]. This validation is based on a large number of stations mainly located at remote sites where tropospheric NO_2 concentrations are low and where the column measurement is dominated by the stratospheric background of NO_2. These surface measurements and retrievals are performed for very low sun conditions and are especially sensitive to the stratosphere. The intercomparison results showed that the SCIAMACHY instrument performance is comparable to GOME. However, because these observations are stratosphere-dominated, and because of the additional retrieval complexities in the troposphere (related to the presence of clouds and aerosols, profile shape assumptions, and inaccuracies of the surface albedo map), these results provide only limited credibility to tropospheric column estimates.

[7] In this paper, we report a new tropospheric retrieval data set for 2003, based on the SCIAMACHY nadir measurements and a retrieval scheme. The SCIAMACHY NO_2 retrievals are used to evaluate the NO_2 fields produced by a new version of the high-resolution regional-scale CHIMERE CTM over western Europe. Since all data have uncertainties, the data are also compared to NO_2 surface observations. The mutual consistency of both SCIAMACHY and CHIMERE outputs over sites where surface measurements are available gives us confidence in both the model and SCIAMACHY over large areas not covered by surface observations. We present comparisons at different timescales (a year, a month, a season, and a day) and on different locations (rural areas, urban areas, and seas).

[8] CHIMERE has a resolution of 50×50 km^2, comparable to the SCIAMACHY footprint size of 30×60 km^2. In this way, comparisons can be made without first degrading the resolution of the satellite observations, as was done in previous studies. The comparison between SCIAMACHY and CHIMERE is performed by collocating the CTM simulations both in space and time to each of the measurement locations of SCIAMACHY, and subsequently applying the averaging kernel [*Eskes and Boersma*, 2003]. Errors related to differences in sampling and a priori profile shape assumptions are therefore minimized as described in the work of *Boersma et al.* [2004].

[9] In section 2, we present the new version of CHIMERE CTM, the surface NO_2 observations, the SCIAMACHY

measurements, and the approach used to compare SCIAMACHY and CHIMERE outputs using the kernels. In section 3, we compare annual means of surface observations, SCIAMACHY NO_2 columns, and CHIMERE surface and column simulations. In section 4, the consistency between the temporal variation of the surface measurements and CHIMERE is evaluated. In section 5, the daily and seasonal variabilities of NO_2 as observed by SCIAMACHY and simulated by CHIMERE are discussed. Section 6 presents the summary and conclusions.

2. Data and Methods

2.1. The CHIMERE Model

[10] CHIMERE is a three-dimensional Eulerian chemistry-transport model. It has been applied over different domains, from the urban scale [e.g., *Vautard et al.*, 2001, 2003a, 2003b; *Menut*, 2003; *Beekmann and Derognat*, 2003; *Blond et al.*, 2003] to the continental scale [e.g., *Blond and Vautard*, 2004; *Bessagnet et al.*, 2004]. These studies evaluate the performance of the model for various species using surface and airborne measurements. At continental scale, the root mean square error (RMSE) of simulated daily maximum ozone mixing ratio, for 115 European surface sites during period for May to September 1998, is reported to be about 10 ppb (for a mean observed mixing ratio of about 50 ppb) [*Schmidt et al.*, 2001]. *Blond and Vautard* [2004] found similar values for RMSE of simulated daily ozone mixing ratio for 15h00 UTC during four consecutive summers (May-September 1999–2002). *Schmidt et al.* [2001] evaluated the daily mean NO_2 mixing ratio. The mean bias for 28 monitoring stations was −0.98 ppb for a mean observed mixing ratio of 3.85 ppb. For a large number of sites, the correlation coefficient was between 0.50 and 0.78. The nested simulation for the Paris area agreed well with observations during summer 1999: In the urban area, simulated and observed ozone maxima show RMSE in the range of 6–10 ppb and correlation coefficients between 0.7 and 0.8 [*Vautard et al.*, 2001]. For the intensive observing period of the ESQUIF campaign [*Menut et al.*, 2000] which has been performed in Paris area during summer 1999, satisfactory model agreement with total nonmethane hydrocarbon (NMHC; average error was lower than 10%) and NO_y (average error was lower than 5%) was noted [*Vautard et al.*, 2003a]. The CHIMERE model is now part of the national air pollution forecasting system in France (Prev'Air). It has also been intercompared to other CTMs over several European cities [*Cuvelier et al.*, 2007].

[11] For this study, we use a continental configuration over western Europe with a horizontal resolution of 0.5° × 0.5°. Domain and grid are shown in Figure 1.

[12] The model formulation is based on the mass continuity equation for several chemical species in every grid cell. The time numerical solver is the TWOSTEP method [*Verwer*, 1994] which is applied to integrate all processes including transport, chemistry, emission, and diffusion as proposed by *Schmidt et al.* [2001]. The time step is 10 min. In this work, we use a vertically extended version of CHIMERE allowing to account for the whole troposphere over western Europe. The new vertical discretization consists of 15 layers from the surface up to 200 hPa with the first layer having a top at 50 m.

[13] The chemical mechanism is the complete MELCHIOR mechanism [*Lattuati*, 1997] which includes 82 gaseous species compounds and 333 reactions. This chemical mechanism has been elaborated for use in photo-oxidant modeling both under polluted and clean air conditions. It is based on the European Monitoring and Evaluation Program (EMEP) mechanism [*Simpson*, 1992] with substantial extensions concerning the NO_3 and organic nitrate chemistry, the degradation of aromatic and biogenic hydrocarbons, and the recombination of organic peroxy radicals. The photolysis rates were computed using the troposphere ultraviolet and visible model (TUV [*Madronich and Flocke*, 1998]), modulated by cloudiness [*ESQUIF*, 2001].

[14] The CTM is driven by the European Center for Medium-Range Weather Forecasts (ECMWF) meteorological short-range forecasts. These data are calculated by a model with a spectral resolution of TL511 and available with a horizontal resolution of about 0.5° × 0.5°. The meteorological fields are provided with a time resolution of 3 hours and are linearly interpolated to 1-hour intervals, including temperature, pressure, wind, humidity, and cloudiness fields. Vertically, the meteorological data given for 18 ECMWF levels are interpolated to CHIMERE levels. The land-use data are derived from the Rijksinstituut voor Volksgezondheid en Milieu (RIVM) database [*van de Velde et al.*, 1994]. The convective fluxes are rediagnosed as in the work of *Olivié et al.* [2004] using the scheme of *Tiedtke* [1989].

[15] Boundary concentrations for the continental setup are fixed for eight species (O_3, NO_x, CO, PAN, CH_4, C_2H_6, HCHO, and HNO_3) using the climatological monthly mean data produced by the global MOZART CTM version 2 [*Horowitz et al.*, 2003].

[16] The anthropogenic emissions are derived from the EMEP annual totals for 2001 [*Vestreng et al.*, 2004] for NO_x, SO_2, CO, and nonmethane volatile organic compounds. They have a horizontal resolution of about 0.5° × 0.5° and are spatially interpolated from the EMEP grid onto the CHIMERE grid. According to *Suutari et al.* [2001], the uncertainties of NO_x annual total emissions range from ±10% to ±30% depending on the European country. Monthly, daily, and hourly emissions are computed by imposing the typical time variations taken from the *Generation of European Emission Data for Episodes (GENEMIS)* [1994] database. Therefore a weekend reduction of emissions is considered. For aircraft, only the emissions at the surface where their contribution is the most important [e.g., *Colvile et al.*, 2001; *Moussiopoulos et al.*, 1997; *Perl et al.*, 1997] are accounted for. The database used for the biogenic volatile organic compounds emissions is described by *Derognat et al.* [2003].

[17] In rural areas, NO emissions from microbial processes may be an important source. Since these emissions strongly depend on temperature, they are processed in the model as biogenic emissions. In soils, NO is produced in a reaction chain of oxidation and reduction from ammonium which is used in fertilizers. CHIMERE uses a European inventory of NO emissions from soil [*Stohl et al.*, 1996]. This inventory estimates that the soil emissions occur during the summer months. In the model, these NO emissions are thus only considered during the period from May to August.

[18] NO_x emissions from lightning are not included in CHIMERE. However, their contribution to the NO_2 tropo-

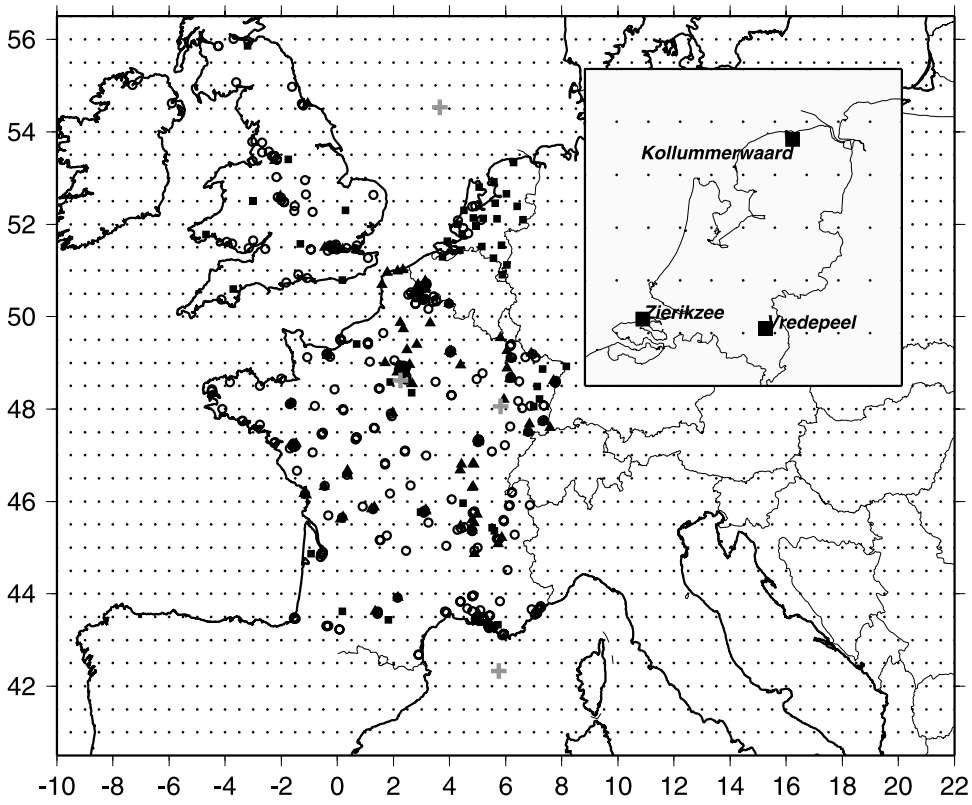

Figure 1. Continental CHIMERE CTM domain and grid, and locations of the 439 NO_2 surface monitoring stations used in this study. Open circles, shaded squares, and triangles denote urban, rural, and suburban stations, respectively. Gray crosses denote locations where vertical profiles of NO_2 mixing ratio and averaging kernels have been extracted. These profiles are shown in Figure 2.

spheric column is small and the comparisons described in this paper focus on cloud-free areas. Using GOME, *Boersma et al.* [2005] found this contribution to be smaller than 0.5×10^{15} molecules/cm^2 in the tropics (observations over large thunderstorms may show enhancements of more than 1e15 molecules/cm^2; however, such events are quite rare over Europe). It is likely smaller over Europe, where lightning is appreciable during summer only. The contribution of lightning to NO_x concentrations is thus only taken into account via the MOZART boundary conditions.

[19] More details about the CTM can be found on the Web site http://euler.lmd.polytechnique.fr/chimere. For the purpose of this study, the model is used to simulate the whole year of 2003.

2.2. NO_2 Surface Measurements

[20] Two main problems encountered when trying to evaluate a continental-scale model with surface observations are (1) the presence of large-extent areas of water without any observations and (2) questionable representativeness of the available observations [*Tilmes and Zimmermann*, 1998] since most of them are located in the vicinity of cities where local sources may have a transient influence which cannot be assessed accurately by a model having a horizontal resolution of 50 × 50 km [e.g., *McNair et al.*, 1996].

[21] Surface measurements of NO_2 used in the present study have been collected from several European air quality monitoring organizations. Observations provided from 439 monitoring stations were available for the analysis. The distribution of monitoring sites is shown in Figure 1. Among these measurements, three different types of monitoring sites can be distinguished corresponding to urban, suburban, and rural stations. The stations of a rural characteristic are assumed to be more representative for a coarse-grid model than the other stations influenced by nearby traffic. Despite their low representativeness, we use suburban and urban stations to evaluate the space-based data over urbanized locations. Observations from these stations are often influenced by local point sources, difficult to simulate in a 50 × 50 km resolution model.

[22] The observations of NO_2 used are issued from a measurement technique that is based first on the conversion of NO_2 to NO, and then subsequent detection of NO using the chemiluminescence method [e.g., *Winer et al.*, 1974]. This method is widely used for continuous monitoring of concentrations in Europe and throughout the world. It has been designed as a reference method by the EU First Air Quality Daughter Directive and the US Environmental Protection Agency. A typical specification is detection limit lower than 1 ppb, precision better than 1%. More information about calibration of the analyzers may be found in the European norm prEN 14211 which is applied by all of the European air quality networks.

[23] However, it is well known that the chemiluminescence method is subject to interferences [e.g., *Winer et al.*, 1974; *Matthews et al.*, 1977; *Rickman and Wright*, 1986]. Two forms of interference may occur in the chemiluminescent sampler: a reduction in the chemiluminescence inten-

sity by quenching in the reaction chamber and bias due to conversion of various N-species to NO taking place in the NO_2-to-NO converter. An assessment of overall uncertainty budgets, including interferences, has been reported by *Gerboles et al.* [2003].

[24] Because of these interferences, the accuracy of NO_2 observations is difficult to estimate. Accuracy is time and location dependent. *Aas et al.* [2000] used different measurement methods to estimate the NO_2 measurement at some selected EMEP sites. The uncertainty has been found to be sometimes larger than 30% (actually for less than 25% of the sites). They also found errors to be less than 10% for some monitoring stations (30% of the EMEP sites). *Ordóèez et al.* [2006] found that a molybdenum converter leads to an overestimation of 20% on measurements of NO_2 in winter compared to measurements performed with a photolytic converter (highly specific technique for NO_2). In summer, they found an overestimation of nearly 50%. On the other hand, RIVM (Dutch air quality agency) observed that most of the other nitrogen components able to interfere with NO_2 measurement have very small concentration levels in Netherlands and will only have a small influence except for ammonia. Because NH_3 concentrations can be substantial, the influence on the measurements could be a few percent. The accuracy for other sites is unknown.

[25] Despite these limitations, NO_2 measurements performed by air quality networks remain the most relevant information to assess NO_2 concentrations in the European boundary layer over large regions. Thus these data will be used in the following sections to characterize the spatial and temporal variability of NO_2 surface concentrations over Europe.

2.3. SCIAMACHY NO_2 Tropospheric Columns

[26] SCIAMACHY is a spectrometer on board ENVISAT ESA satellite that was launched in March 2002. SCIAMACHY measures in the ultraviolet, visible, and near-infrared wavelength ranges. The sensor alternatively scans in the nadir and limb viewing directions and has a local overpass time of approximately 10h00 UTC in western Europe. Individual nadir pixels cover a surface area of 30×60 km^2, and SCIAMACHY achieves global coverage every 6 days.

[27] The SCIAMACHY NO_2 tropospheric column data set presented in this paper is the result of a collaboration between the Belgian Institute for Space Aeronomy (BIRA-IASB) and the Royal Netherlands Meteorological Institute (KNMI), in the framework of the ESA Data User Program Tropospheric Emission Monitoring Internet Service (TEMIS) project. Data sets are available on the TEMIS project web site (http://www.temis.nl).

[28] The first step in retrieving tropospheric NO_2 is performed by BIRA-IASB and covers the spectral fitting of SCIAMACHY Level 1 data to generate so-called slant column densities. The spectral fitting technique used to retrieve total NO_2 slant columns from SCIAMACHY measurements is differential optical absorption spectroscopy (DOAS) [*Platt*, 1994]. A nonlinear least squares inversion based on the Marquardt-Levenberg method is used to minimize residuals between observed and calculated spectra over the wavelength region from 426.3 to 451.3 nm. The measurements are decomposed in a solar irradiance spectrum, measured reference spectrum for NO_2 at 243 K [*Bogumil et al.*, 1999], O_3 at 223 K [*Bogumil et al.*, 1999], O_2-O_2 [*Greenblatt et al.*, 1990], H_2O [*Rothman*, 1992], and a polynomial of the second order. An undersampling cross section and Ring effect cross section [*Chance*, 1998; *Vountas et al.*, 1998] are included as additional pseudo-absorbers.

[29] The second step in retrieving tropospheric NO_2 is performed by KNMI and involves the correction for stratospheric NO_2 and the air mass factor correction [*Martin et al.*, 2002; *Boersma et al.*, 2004]. To account for the temperature dependence of the NO_2 absorption cross sections, a temperature correction is calculated using ECMWF temperature analyses and Tracer Model version 3 (TM3, [*Dentener et al.*, 2002]) modeling results of the NO_2 vertical distribution. Height-dependent air mass factor lookup tables are based on calculations with the Doubling-Adding KNMI (DAK) radiative transfer model [*de Haan et al.*, 1987; *Stammes et al.*, 1989; *Stammes*, 2001] that includes a sphericity correction. The NO_2 stratospheric column is deduced from a TM3 assimilation run of the SCIAMACHY NO_2 slant column data. The assimilated-analyzed stratospheric slant column is then subtracted from the retrieved DOAS total slant column provided by BIRA-IASB, resulting in a tropospheric slant column. Then the tropospheric vertical column is retrieved using TM3 tropospheric model profiles (colocated for each SCIAMACHY pixel individually) and combined with cloud information. The latter consists of cloud fraction and cloud top height derived by the Fresco algorithm [*Koelemeijer et al.*, 2001]. The retrieval includes surface albedo values constructed by using a combination (on a monthly basis) of seasonal minimum reflectivity values derived from 14 years of TOMS reflectivity data [*Herman and Celarier*, 1997] and a database of spectral surface reflectivity derived from 5.5 years of GOME observations [*Koelemeijer et al.*, 2003]. No aerosol correction is applied: This choice is based on the recognition that the cloud retrieval will be influenced by aerosol as well and is further motivated by the error analysis presented in the work of *Boersma et al.* [2004]. The NO_2 column data products are provided on the TEMIS web site with detailed error estimates and kernel information [*Eskes and Boersma*, 2003].

[30] In this study, we use only observations where the radiance of the cloud-covered part of the SCIAMACHY footprint contributes less than 50% to the total radiance, which roughly corresponds to cloud fractions below 10–15%. Snow-covered scenes are also excluded from the analysis. The observations are available at about 10h00 UTC. The individual retrievals have a typical precision of 35–60% over Europe. This uncertainty is dominated by the uncertainty in the estimate of the tropospheric air mass factor. The most important uncertainties associated with the computation of the tropospheric air mass factor are cloud fraction, aerosol characterization, surface albedo, and profile shape. More information about the retrieval method and the estimate of the uncertainties can be found in the work of *Boersma et al.* [2004].

2.4. SCIAMACHY and CHIMERE Intercomparison Approach

[31] The comparison between SCIAMACHY NO_2 column observations and the NO_2 simulated fields consists of a model-to-observation approach of three steps. In step 1,

CHIMERE simulations are interpolated in time and space to produce vertical NO_2 profiles $\mathbf{x}_c(k, t)$ at each of the SCIAMACHY measurement locations k (centers of the SCIAMACHY pixels) and times t. In step 2, the averaging kernel vector $\mathbf{A}$ of the retrieval is applied to the model profile to produce a model prediction of the retrieved column $z_c(k, t)$, to be compared with the SCIAMACHY retrieved total NO_2 column, $y_c(k, t)$,

$$z_c(k,t) = \mathbf{A}(k,t) \cdot \mathbf{x}_c(k,t). \quad (1)$$

In step 3, we compute the error statistics. For individual days, comparisons are done at the SCIAMACHY measurement locations. For seasonal and annual mean comparisons, we regrid both the CHIMERE and SCIAMACHY columns to a common $0.5^\circ \times 0.5^\circ$ grid, where the averaging is based on weighted according to the spatial fraction of the SCIAMACHY pixel size within a grid cell.

[32] This model-to-observation approach makes the comparison independent of profile shape assumptions needed in the retrieval (as discussed extensively in the work of *Eskes and Boersma* [2003] and *Boersma et al.* [2004]). Indeed, the retrieval of tropospheric NO_2 depends on a priori assumptions on the vertical profile of NO_2 in the troposphere. In our retrievals, these profiles are taken from simulations with the global TM3 CTM (as described in section 2.3). Systematic errors in these modeled profile shapes will result in errors in the retrieved column estimated to be of the order of 5–15% [*Boersma et al.*, 2004]. Applying the SCIAMACHY averaging kernel to the CHIMERE profile consists of retracing the retrieval steps. The comparison between the resulting model prediction of the retrieved column and the SCIAMACHY retrieved column itself is then no longer influenced by possible errors in the TM3 a priori profile shapes (more details can be found in the work of *Eskes and Boersma* and *Boersma et al.*).

[33] In Figure 2, we show four typical NO_2 profiles simulated by CHIMERE and the corresponding four averaging kernels. These profiles were selected over a polluted area (over Paris, Figure 2a), over three nonpolluted areas (over the northeast of France, Figure 2b; over the Mediterranean Sea, Figure 2c; over the North Sea, Figure 2d; see locations in Figure 1). At 10h00 UTC, the boundary layer is quite well mixed, but significant gradients remain between the surface and the top of the boundary layer. In certain cases, there is a substantial NO_x contribution above the boundary layer. The kernels show that the satellite has a lower sensitivity at the surface due to the partial cloud coverage and to the generally low albedo of the surface [*Eskes and Boersma*, 2003].

3. Spatial Comparison of Surface Measurements, SCIAMACHY, and CHIMERE NO_2

[34] Annual means of surface NO_2 observations, surface NO_2 simulations, model NO_2 tropospheric columns, and SCIAMACHY NO_2 tropospheric columns are compared in Figure 3. The aim of this comparison is to investigate how the modeled spatial NO_2 distribution matches the observations. The averages are computed over the whole year 2003 but have been restricted to days when surface observations and SCIAMACHY data were simultaneously available in a model grid box. In these cases, we compute the grid box mean of the surface observations, the SCIAMACHY data, and the CHIMERE simulations. We obtain a total of 176 grid boxes. Given the daily SCIAMACHY coverage and the given cloudiness criterion, not all possible days have valid data. The number of days included in the averages varies between 1 and 20.

[35] Figure 3a compares surface NO_2 observations with surface NO_2 simulations (i.e., the simulated concentrations for the first layer of the model). The correlation coefficient for the complete set of stations is low (0.55, $n = 176$). The subset of sites along the 1:1 line mostly denotes rural and suburban sites. The large subset of sites where the model simulations range from 1 to 3 ppb while, at the same time, the observations range from 8 to 17 ppb mostly corresponds to urban sites where the model often underestimates the surface NO_2 (slope is 0.38). When restricted to rural sites (Figure 3e), the correlation coefficient between surface measurements and simulated concentrations is significantly improved, 0.83 ($n = 29$), and the slope is closer to 1 (0.68).

[36] A large part of the bias noted on urban sites may be attributed to the low horizontal resolution of the model. Indeed, surface NO_2 gradients are very large inside and in the vicinity of cities, and local measurements are difficult to link to the concentrations simulated over a model grid mesh as large as 50×50 km^2. Similar simulations have been performed over the Alsace region (northeast of France on the border France-Germany) with a regional version of the CHIMERE model using a higher horizontal resolution (3×3 km^2). Only the horizontal resolution of the emissions (3×3 km^2) has been increased. The meteorological data have been interpolated. These new simulations show that the model underestimations noted on NO_2 concentrations are largely reduced. These reductions reach 5% on rural sites, 16% on suburban sites, and 80% on urban sites. In Figure 3b, the observed surface NO_2 concentrations are plotted against the SCIAMACHY tropospheric columns. The correlation coefficient is again low (0.43, $n = 176$). As for CHIMERE, the resolution of SCIAMACHY (30×60 km^2) does not match with local measurements performed in areas where strong spatial gradients of NO_2 exist. When the comparison is limited to rural sites (Figure 3f), the correlation coefficient is again much larger (0.90, $n = 29$).

[37] These results show that NO_2 surface measurements performed in urban areas cannot be used for the validation of the SCIAMACHY NO_2 tropospheric columns or for that of a regional-scale CTM with a relatively low spatial resolution. They also show that for rural areas, there is a direct relationship between the measured NO_2 surface concentrations and both (boundary layer integrated) SCIAMACHY total columns and CHIMERE NO_2 simulated concentrations.

[38] Figure 3c compares NO_2 model and SCIAMACHY annual mean tropospheric columns. The correlation coefficient is high (0.88) showing that the mean spatial distribution of the NO_2 model and SCIAMACHY tropospheric columns are quite consistent. It should be noted that the NO_2 tropospheric columns are in good agreement both in rural and urban areas. However, the model tends to underestimate the highest SCIAMACHY values, which results in a regression slope of 0.71. We note that the largest differences between observed and simulated columns often correspond to averages computed for samples of less than

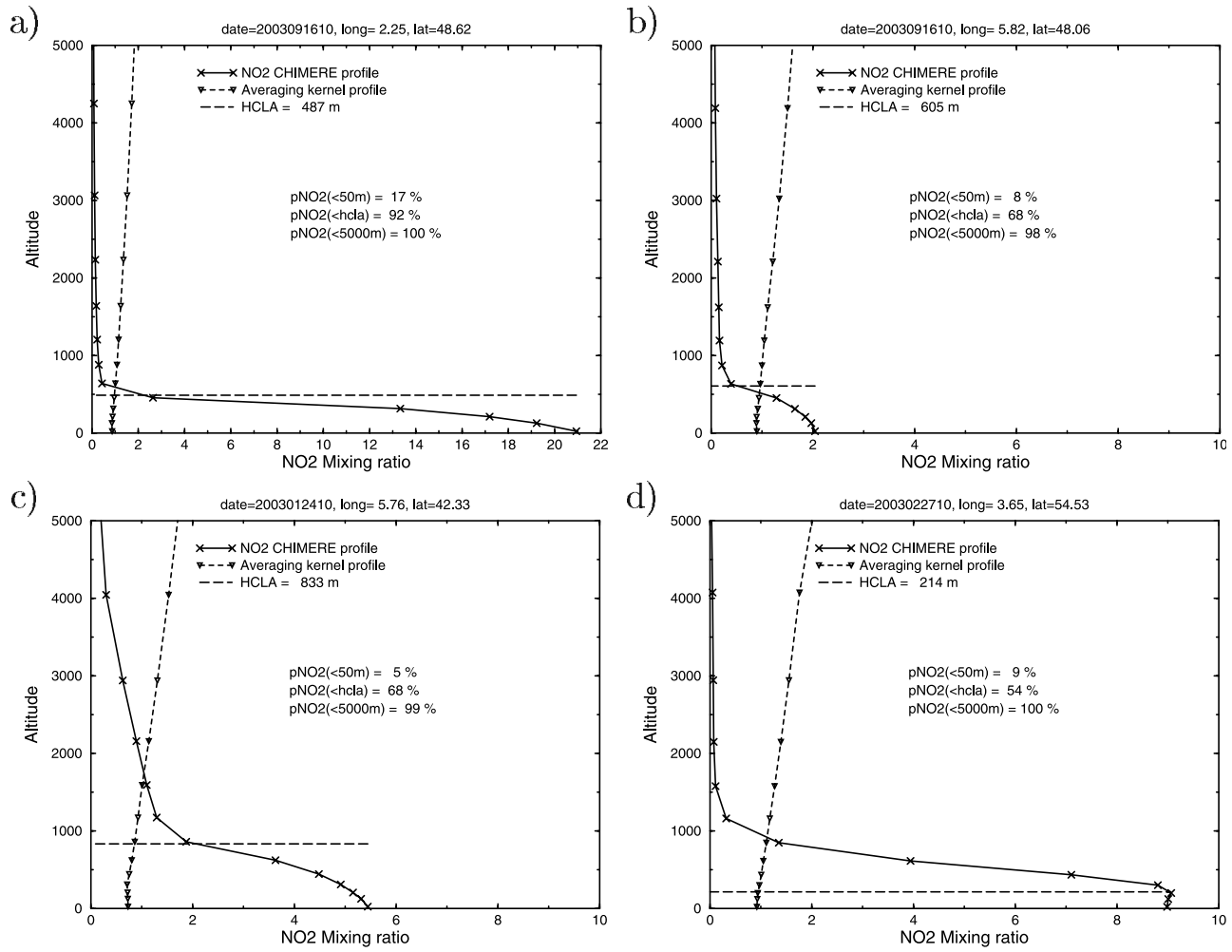

Figure 2. Vertical profiles of NO_2 mixing ratio over (a) Paris area, (b) northeast of France, (c) Mediterranean Sea, (d) North Sea (see locations in Figure 1). The solid line and the crosses show the NO_2 profile simulated by CHIMERE. The dashed line and the triangles show the profile of the averaging kernels. The dashed line indicates the height of the boundary layer (HCLA). pNO_2(<50 m), pNO_2(<hcla), and pNO_2(<5000 m) give the percentage of NO_2 mass in the first 50 m, in the boundary layer, and below 5 km, respectively. NO_2 mixing ratios are in ppb. Altitude in meters.

5 collocated measurements showing that it is more difficult to simulate individual NO_2 values than mean values. When we do not consider these cases, slope and correlation are closer to 1 (0.76 and 0.92, respectively).

[39] In Figure 3d, surface NO_2 simulations are plotted against SCIAMACHY NO_2 tropospheric columns. The correlation coefficient is again high (0.85, $n = 176$) suggesting that, on a yearly basis, the spatial distribution of observed tropospheric column of NO_2 is very representative of the distribution observed in the surface concentrations, and that lower correlations obtained with surface in situ observations are due to urban small-scale variability.

4. Temporal Comparison of Surface-Level NO_2

[40] In this section, we present the results of the comparison between time series of daily NO_2 surface observations and simulated NO_2 surface concentrations collected for 10h00 UTC (the approximate measurement time of SCIAMACHY) over the whole year 2003. Table 1 lists the simulation-minus-observation error statistics averaged for station categories (urban, suburban, rural) for French, Dutch, and British monitoring stations.

[41] Systematic biases vary from −10.2 to +3.3 ppb on average, showing the general CTM tendency to underestimate NO_2 surface measurements in the urban and suburban areas and slightly to overestimate these measurements in the rural areas. The CTM underestimations in urban and suburban areas are likely related to the low horizontal resolution of the model as explained in section 3. In general, NO_2 gradients are smoothed: lowest mixing ratios are slightly overestimated and the highest are largely underestimated. This is why the regression slope is lower than 1 (between 0.25 and 0.70) and the RMSE is quite high compared to the mean values (50–100%). For rural stations, the CTM overestimates the NO_2 measurements of less than 7% over Netherlands and the Greater Paris Region. These overestimations reach 49% over the United Kingdom where most of rural stations are located in altitude. For French rural stations, the CTM slightly underestimates the NO_2 measurements. Since these measurements are known to overestimate

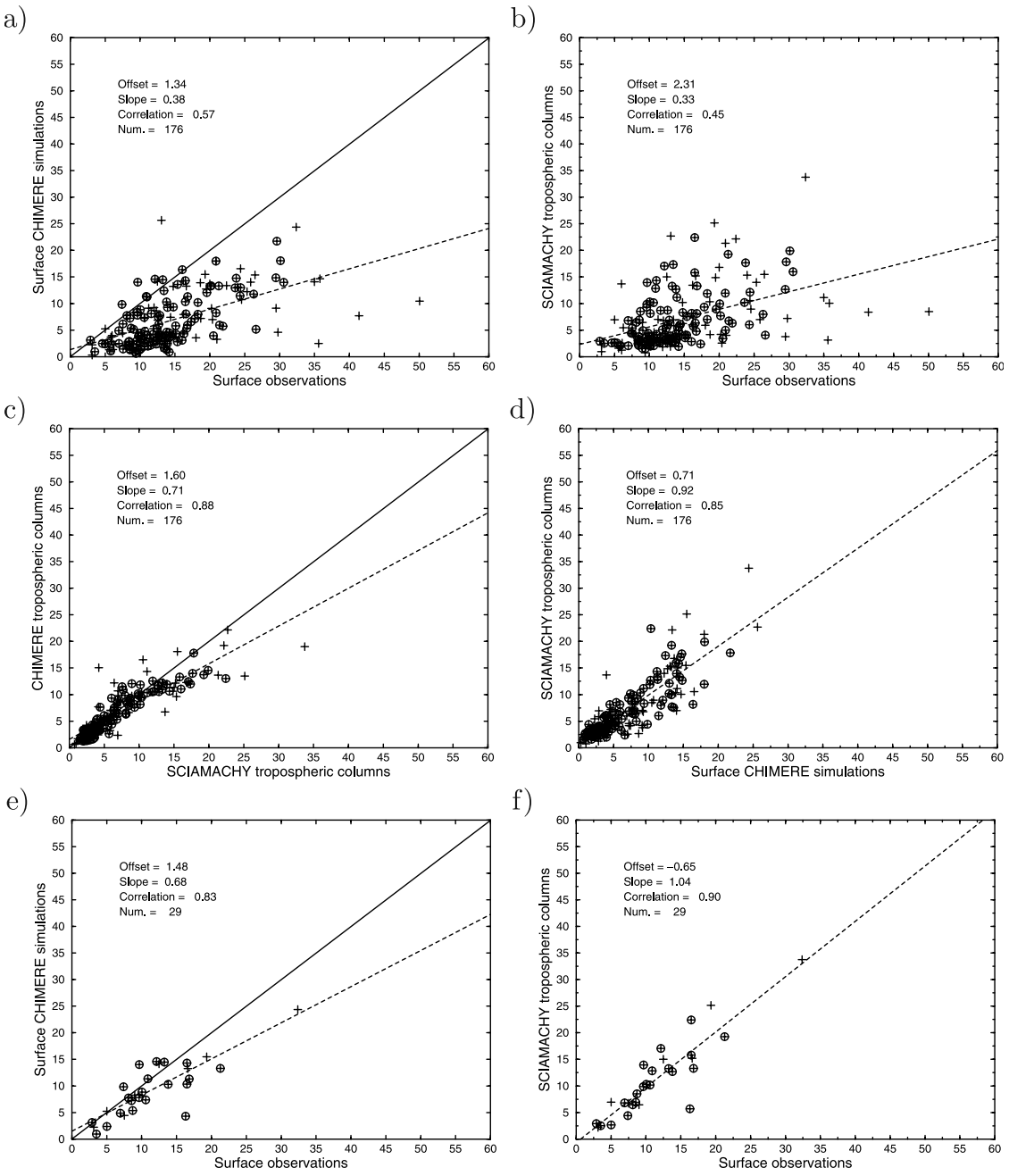

Figure 3. Comparison of annual means of (a) surface NO_2 observations and surface NO_2 CHIMERE simulations, (b) surface NO_2 observations and SCIAMACHY NO_2 tropospheric columns, (c) NO_2 SCIAMACHY and CHIMERE tropospheric columns, (d) surface NO_2 CHIMERE simulations and SCIAMACHY NO_2 tropospheric columns. Figures 3e and 3f are same as Figures 3a and 3b, respectively, but surface observations have been restricted to rural sites. Surface observations and simulations are in ppb. NO_2 columns are in 10^{15} molecules/cm^2. Circles denote means computed over more than 5 days.

the true NO_2 concentrations (20% in average, see section 2.2) in the rural areas, the underestimations are not a sign of model error but could be due to an observation bias. However, the overestimations are an indication that the CTM overestimates the true NO_2 concentrations. These overestimations are estimated to be less than 30% at the surface. In order to evaluate the seasonality of the bias, we computed the mean bias for spring-summer and autumn-winter periods on rural and urban sites. On rural sites, this bias is of 6% for spring-summer and 21% for autumn-winter. Since during the warm season, the photochemistry leads to higher production of secondary pollutants than in autumn-winter and consequently to a more pronounced overestimation of the NO_2 surface concentrations by ground measurements, the NO_2 surface concentrations are clearly more overestimated by the CTM in autumn-winter than in spring-summer. On urban sites, the mean bias is −43% for spring-summer and −37% for autumn-winter. Taking into account the potential measurement errors, no conclusions may be given.

Table 1. Statistics Derived From the Comparison of NO_2 Tropospheric Columns Simulated by CHIMERE and Those Measured by SCIAMACHY (No Data Were Available for November)[a]

Period	Bias	RMSE	Offset	Slope	COR	CORem	OBS	SIM	Num.
Year	−0.2/−5	1.7/45	0.6	0.77	0.87	0.72	3.8	3.6	2003
Winter	0.5/7	4.5/64	3.2	0.62	0.79	0.48	7.0	7.5	1078
Spring	−0.7/−17	2.6/62	1.0	0.59	0.77	0.67	4.2	3.5	1766
Summer	−0.6/−19	1.6/52	0.2	0.73	0.82	0.74	3.1	2.4	1779
Autumn	0.7/23	1.8/60	1.1	0.87	0.83	0.67	3.0	3.7	1739
December	1.9/42	4.4/98	3.8	0.59	0.65	0.14	4.5	6.5	347
January	1.9/37	4.0/78	3.0	0.78	0.71	0.29	5.1	7.0	343
February	−0.3/−4	4.8/59	2.8	0.62	0.82	0.52	8.1	7.8	761
March	0.7/19	2.7/75	1.6	0.73	0.75	0.63	3.6	4.2	1119
April	−1.6/−29	3.9/71	1.4	0.44	0.77	0.60	5.5	3.9	1178
May	−0.9/−25	2.4/67	0.5	0.60	0.76	0.66	3.6	2.7	1218
June	−0.9/−29	2.1/68	0.5	0.56	0.73	0.62	3.1	2.3	1437
July	−0.3/−10	1.8/62	0.4	0.76	0.77	0.69	2.9	2.6	1351
August	−0.5/−18	1.5/54	0.5	0.66	0.80	0.70	2.8	2.3	1176
September	0.3/10	1.6/53	1.0	0.78	0.85	0.70	3.0	3.3	1515
October	1.1/35	2.3/74	1.5	0.89	0.76	0.57	3.1	4.2	1171

[a]The bias is given in absolute value and in percent (relative to the mean observation). RMSE is the root mean square of the simulation-minus-observation residuals, also given in absolute value and in percent (relative to the mean observation). COR is the spatial and time correlation coefficient computed between observations and simulations. CORem is the spatial and time correlation coefficient computed between observations and emissions. Slope and offset are the coefficients of a linear fit of the plot of observations versus simulations. OBS is the mean of the observed values, SIM that of the CHIMERE simulated values. Columns are in 10^{15} molecules/cm^2, emissions in 10^{10} molecules cm^{-2} s^{-1}.

[42] The mean correlation coefficients are around 0.6 ($n \simeq 300$) showing the general problem to simulate the temporal variability of NO_2 concentrations. Differences may be due to deficiencies in the model (the difficulty to simulate vertical NO_2 gradient during the rise of the boundary layer) or in model inputs (uncertainty on clouds and the NO_x emissions [*Hanna et al.*, 1998; *Kuhlwein and Friedrich*, 2000; *Suutari et al.*, 2001; *Beekmann and Derognat*, 2003]) but are also related to the limited accuracy and representativeness of surface measurements (for example, discussion in section 2.2). Higher correlations for Paris and Dutch rural stations are an indication of the role of representativeness. Indeed, these stations are located far away from local emission sources but are often influenced by large pollution plumes. Most of Dutch stations are in the south of Netherlands and are often influenced by the pollution episodes which frequently occur in the Ruhr and the Benelux (the means of the NO_2 surface observations and simulations at these stations are around 13 ppb; they are around 8 ppb for the rural French and British stations). Netherlands and Paris areas are also very flat, and the high scores may be also partly due to a reduction of orography-induced modeling errors.

[43] Figure 4 shows time series of daily 10h00 UTC NO_2 concentrations observed and simulated from 1 January to 31 December 2003 for a selection of monitoring sites. These monitoring stations have been selected because they are assumed to be representative of the model grid cell: one is in United Kingdom (London-Bexley, urban station), one is near Paris in France (Foret de Rambouillet, rural station), and the last three others are rural stations located in several regions of Netherlands. Zierikzee is located in the southwest of Netherlands, Vredepeel in the southeast, and Kollumerwaard, near the sea coast in the north of the country (cf. Figure 1).

[44] The CTM represents most of the day-to-day variability of NO_2 over all of the observation stations (stations located in rural areas, in urban area, and near the sea). It captures most of the NO_2 peaks, but there are some underestimations. On 16 April, the underestimations reach 5–10 ppb for three of the monitoring stations located in London, near Paris, and in Netherlands. These errors suggest that there is a problem on a large scale.

[45] The NO_2 south-north and west-east gradients frequently observed in Netherlands are also well captured by the CTM. The gradient of NO_2 concentration in the south-north direction can be seen for instance for 27 February, 28 March, and 16 September. Observations given by monitoring stations, Zierikzee and Vredepeel, located in the south of Netherlands, are often correlated. However, during the beginning of June, the extension of the NO_2 plume centered the Ruhr, and the Benelux was small and only Zierikzee recorded high concentrations. The CTM well captures this west-east gradient but misses to simulate the highest peak occurred for 7 June on station Zierikzee. This peak is actually simulated by the CTM more to the north.

[46] Above all, these results show that the model is able to simulate the time variations of NO_2 in rural areas, far from sources (the correlation coefficients are larger than 0.70). They also show that the CTM probably tends to overestimate the true NO_2 concentrations at the surface in the rural locations.

5. Comparisons Between CHIMERE and SCIAMACHY NO_2 Tropospheric Columns

[47] In this section, we investigate the consistency of the spatial and temporal variabilities of NO_2 tropospheric columns measured by SCIAMACHY and simulated by CHIMERE. We show maps and error statistics computed for the whole year 2003, individual months, and days. The results presented are restricted to nearly cloud-free pixels. Snow-covered scenes are also excluded from the analysis.

5.1. Yearly Mean Comparison

[48] Figures 5a and 5b are maps of the annual means of the NO_2 tropospheric columns over Europe as observed by

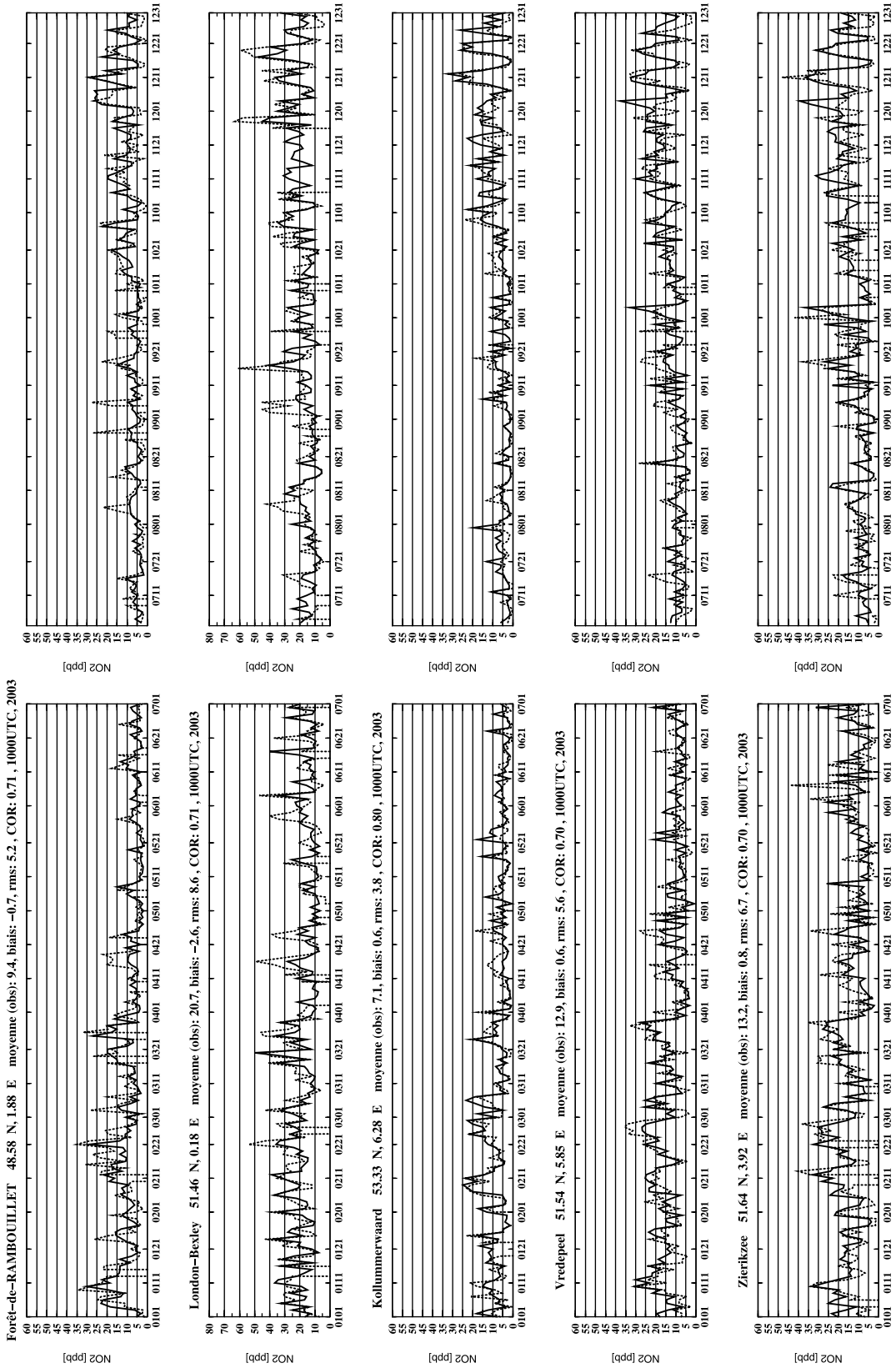

Figure 4. Time series of daily NO_2 mixing ratios in ppb from 1 January to 31 December 2003 taken at 10h00 UTC. Dashed line: observations; solid black line: simulations. The figure title contains the name and the geographical location of the respective observation sites, mean of the observed data, biases, RMSE, and the corresponding correlation coefficients.

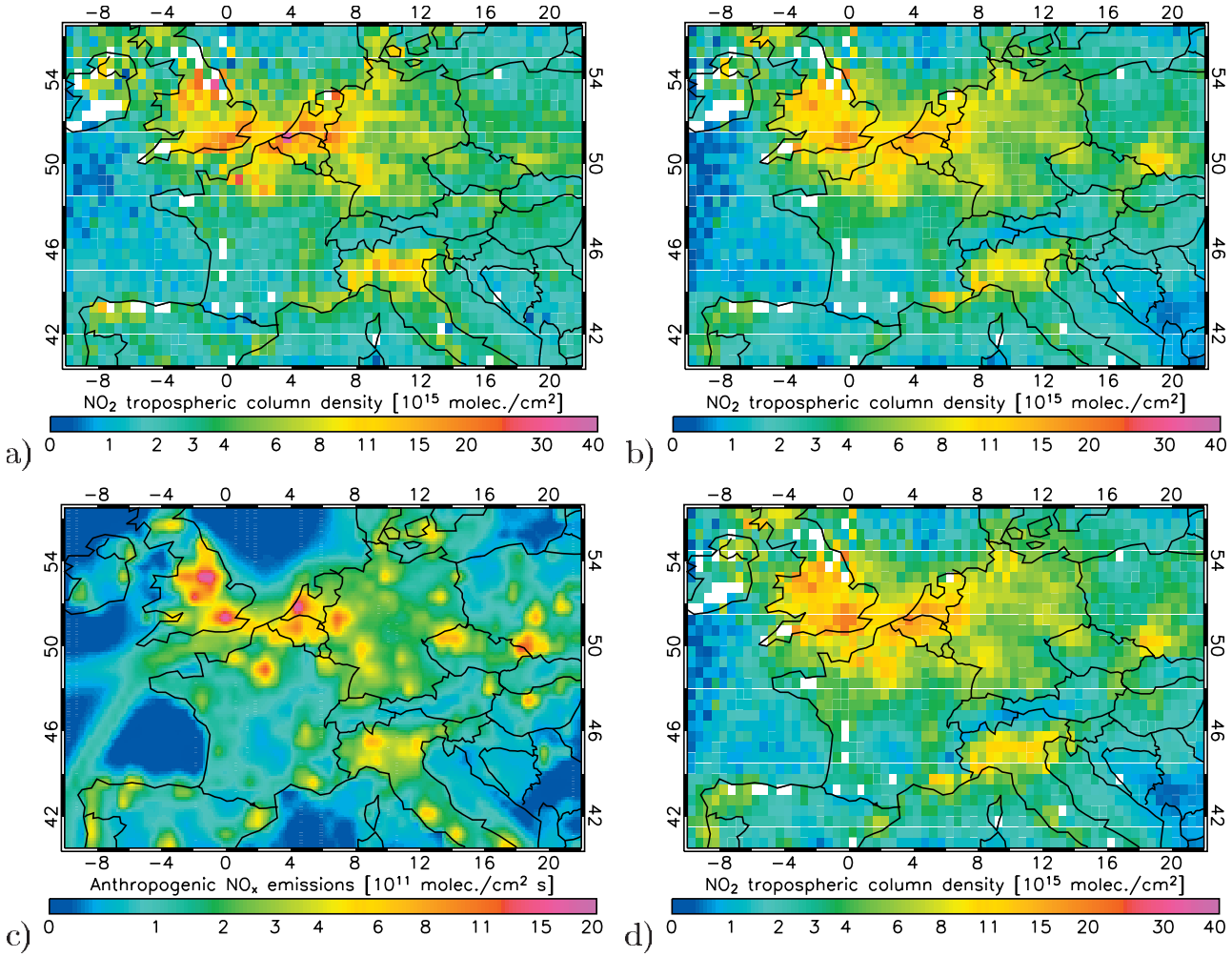

Figure 5. Comparisons between annual means of (a) NO_2 SCIAMACHY tropospheric columns (10^{15} molecules/cm^2), (b) NO_2 CHIMERE tropospheric columns obtained by using the averaging kernels, (c) emissions of nitrogen oxides (NO_x) over western Europe for 10h00 UTC for year 1998, and (d) NO_2 CHIMERE tropospheric columns computed without using the averaging kernels. The emissions are derived from data given by EMEP [*Vestreng et al.*, 2004], interpolated on the CHIMERE grid domain, unit 10^{10} molecules cm^{-2} s^{-1}.

SCIAMACHY and simulated by CHIMERE, respectively. There is a general good agreement between CHIMERE and SCIAMACHY both concerning the spatial distribution and the absolute values. Note that the NO_2 values span 2 orders of magnitude.

[49] Figure 5c illustrates the spatial distribution of the NO_x annual anthropogenic emissions for 10h00 UTC over western Europe, as used in CHIMERE. The largest NO_x emissions are especially located over the Benelux, the Ruhr area, England, and the Po Valley.

[50] When compared with Figure 5c, Figures 5a and 5b show that on an annual average, the NO_2 spatial distribution bears similarities with the NO_x emission spatial distribution. The correlation coefficient between SCIAMACHY observations and the NO_2 emissions is 0.72 (n = 2003) for the whole year. The comparisons also show that the CTM tends to underestimate SCIAMACHY NO_2 values in areas with the largest anthropogenic NO_x emissions, except in the Katowice area (the main emission area in Poland) and over the Etang de Berre (a large industrial area near Marseilles).

[51] In order to study the sensitivity to the retrieval averaging kernels, Figure 5d presents the annual mean of NO_2 CHIMERE tropospheric columns computed without using the averaging kernels. When compared with Figure 5b, Figure 5d shows that the yearly mean-kernel-multiplied and direct CHIMERE tropospheric NO_2 columns are quite similar. *Boersma et al.* [2004] estimated that differences in the amount of mixing in the boundary layer and profile variability can lead to changes in the retrieval of about 5–15%. The differences observed between the yearly mean-kernel-multiplied and direct CHIMERE tropospheric NO_2 columns are smaller, demonstrating a consistency of the profile shapes between CHIMERE (0.5° × 0.5°) and TM3 (2° × 3°). Since CHIMERE has a much higher resolution than TM3, one expects larger differences between the simulated profile shapes for individual times and locations.

[52] Table 2 summarizes the quantitative results of the comparison. The correlation coefficient (0.87) is high for the whole year 2003. The bias is about 5% of the mean value of observed NO_2 columns. The RMSE reaches 45%.

Table 2. Statistical Indicators for Time Series Comparisons of NO_2 Surface Observations and NO_2 Surface CHIMERE Simulations Collected for 10h00 UTC Over the Whole Year 2003[a]

	Bias	RMSE	Offset	Slope	COR	OBS	SIM	Num.
France								
Rural Stations	−1.0/−12	5.5/64	3.4	0.48	0.58	8.6	7.6	336
Suburban Stations	−4.4/−34	8.5/66	4.0	0.35	0.58	12.9	8.6	329
Urban Stations	−9.4/−57	12.7/77	3.2	0.25	0.56	16.6	7.2	332
United Kingdom								
Rural Stations	3.3/49	6.9/101	5.5	0.70	0.59	6.8	10.1	227
Urban Stations	−7.7/−38	12.2/61	4.3	0.42	0.59	20.0	12.3	317
Netherlands								
Rural Stations	0.9/7	6.4/50	5.7	0.65	0.68	12.8	13.7	324
Urban Stations	−5.5/−24	11.4/51	8.0	0.40	0.60	22.5	16.9	340
Greater Paris Region								
Rural Stations	0.3/4	4.8/59	3.8	0.57	0.70	8.1	8.4	340
Suburban Stations	−4.2/−26	9.2/57	5.7	0.39	0.65	16.1	12.0	340
Urban Stations	−10.2/−42	15.4/63	7.0	0.30	0.62	24.4	14.2	312

[a]The bias is given in absolute value and in percent (relative to the mean observation). RMSE is the root mean square of the simulation-minus-observation residuals, also given in absolute value and in percent (relative to the mean observation). COR is the correlation coefficient computed between time series of observations and simulations. OBS is the mean of the observed values, SIM that of the CHIMERE simulated values. Error statistics are averaged over station types (urban, suburban, and rural). Concentrations are in ppb.

The positive offset and the low slope (0.77) indicate that SCIAMACHY measurements have a larger range of values than the CHIMERE simulations. These statistic values are slightly different from the statistics obtained in section 3 because the comparison is here not only restricted to the surface observation locations but also concerns areas not covered by surface measurements.

5.2. Seasonal and Monthly Comparison

[53] Table 2 also gives error statistics for the four seasons and the individual months. The correlation coefficients always have high values ranging from 0.65 to 0.85 for all the months. The means of SCIAMACHY data and CHIMERE simulations agree within less than 23%. SCIAMACHY and simulated mean columns both show that NO_2 tropospheric values are higher during winter than summer. However, the CTM tends to overestimate SCIAMACHY data during autumn-winter (positive biases of 7–23%) and to underestimate them during spring-summer (negative biases of 17–19%). The RMSE values show that the differences between individual CTM outputs and SCIAMACHY observations are slightly larger in winter (about 60% of the mean SCIAMACHY columns) than in summer (50%).

[54] These results may be compared to other studies performed over Europe showing monthly comparisons between simulated and observed NO_2 tropospheric columns. *Konovalov et al.* [2004] found that CHIMERE (version with a model top at 500 hPa) underestimates GOME data during summers 1997 and 2001 with a negative biases of 23% and 33%, respectively. They explained these negative biases by the omission of the upper troposphere. Compared to *Konovalov et al.* [2004], the negative biases are smaller in our study. This result suggests a positive impact of the extended version of CHIMERE with an upper level at 200 hPa. As discussed by *Vautard et al.* [2005], a possible overestimation of the dry deposition during spring-summer 2003 may be of relevance to explain the residual underestimations for this year. Indeed, spring and summer 2003 were characterized by an exceptionally high temperature and a precipitation deficit leading to an important decrease in dry deposition. The dependence of the dry deposition with water deficit is not taken into account in CHIMERE. This leads to a probable dry deposition overestimation. *Lauer et al.* [2002] found strong positive differences (165% in average) over Europe between the monthly means simulated by the general circulation model ECHAM4.L39(DLR)/CHEM and issued from GOME. *Savage et al.* [2004] also found strong positive differences (90% in average) between the monthly means simulated global CTM TOMCAT and issued from GOME. In these last two studies, the potential source of errors in simulated and observed NO_2 tropospheric columns has been discussed in detail. *Savage et al.* [2004] concluded that the noted overestimations are probably due to weaknesses in their model treatment of vertical mixing and chemistry (limited NMHC chemistry and lack of the hydrolysis of N_2O_5 on tropospheric aerosols). In order to explain the large overestimations, *Lauer et al.* [2002] also pointed out the lack in the CTM of the hydrolysis of N_2O_5 on tropospheric aerosols. *Dentener and Crutzen* [1993] showed that this additional NO_x sink reduces the NO_x present in the boundary layer at middle latitude by up to 80% in winter and 20% in summer. CHIMERE only includes a N_2O_5 loss with humidity (following the results of *Mentel et al.* [1996]). Taking into account an additional NO_x sink induced by the presence of aerosols may improve the comparisons. Differences between our results and the others may be also explained by the use of different emission databases, CTMs (global or regional), satellite data, and retrieval methods.

[55] Figure 6 shows a comparison of seasonal means (winter, spring, summer, and autumn) of both SCIAMACHY and CHIMERE NO_2 tropospheric columns. During winter 2003, only limited number of SCIAMACHY data were available, resulting in data gaps in Figure 6a.

[56] The NO_2 tropospheric columns from CHIMERE and SCIAMACHY exhibit similar spatial structure with similar areas associated to higher and lower NO_2 tropospheric columns. The seasonal pattern is consistent with higher contents of the NO_2 tropospheric columns in winter than in summer. However, the spatial variability of the NO_2 tropospheric columns is greater for SCIAMACHY than for CHIMERE, leading simultaneously to high correlation and

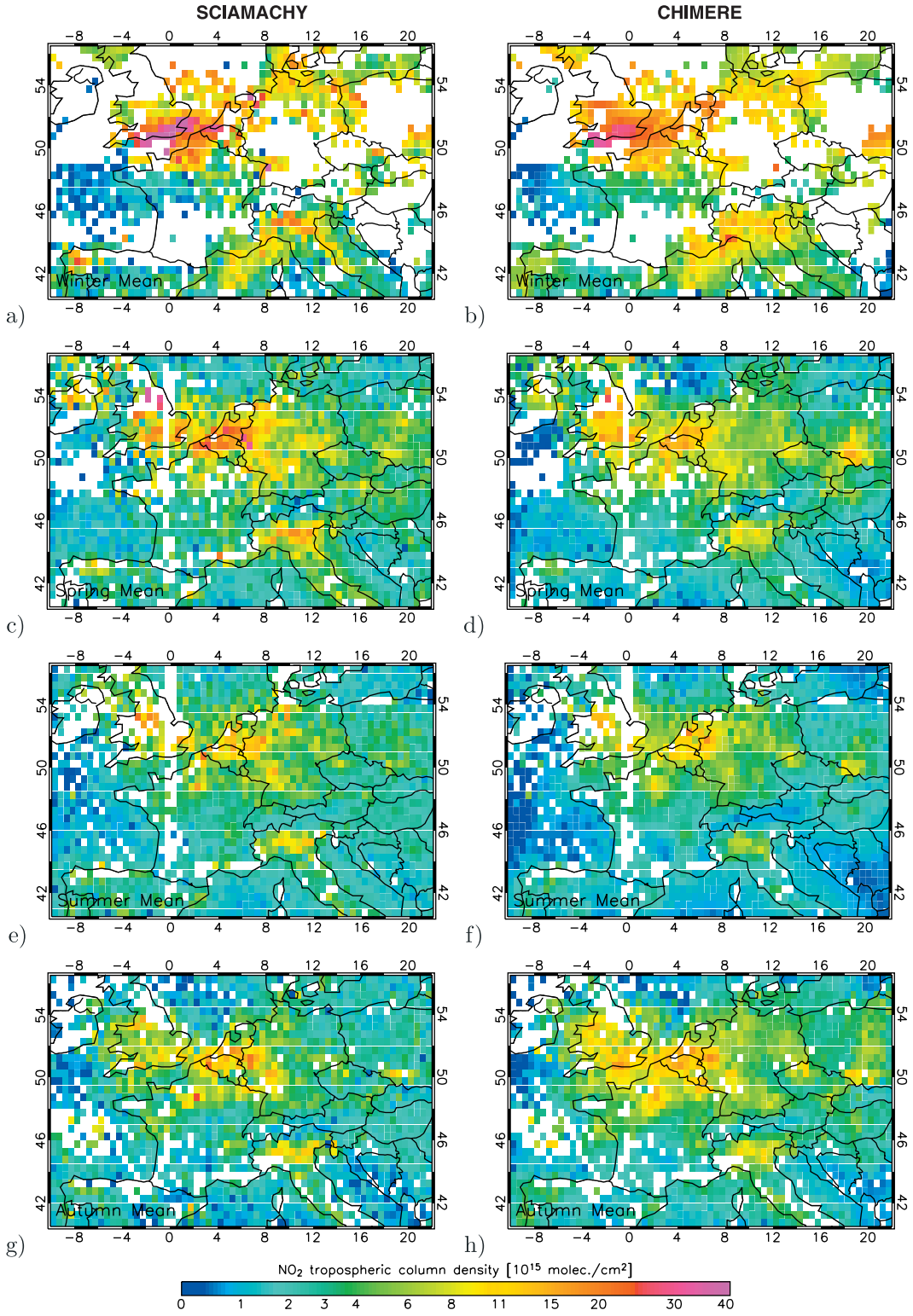

Figure 6. Comparisons between NO_2 SCIAMACHY tropospheric columns on the left and NO_2 CHIMERE tropospheric columns on the right, for (a, b) winter 2003, (c, d) spring 2003, (e, f) summer 2003, autumn 2003, 10h00 UTC. Unity in 10^{15} molecules/cm^2.

high RMSE (see Table 2). In the same way, a stronger seasonal variability is observed with SCIAMACHY over most of the highest NO_x emissions areas (Ruhr and the Benelux, Po-Valley, England). Especially over these intense emission areas, CHIMERE tends to underestimate the NO_2 SCIAMACHY columns. Moreover, during winter and autumn, the CTM overestimates the lowest NO_2 SCIAMACHY columns, while during summer and spring,

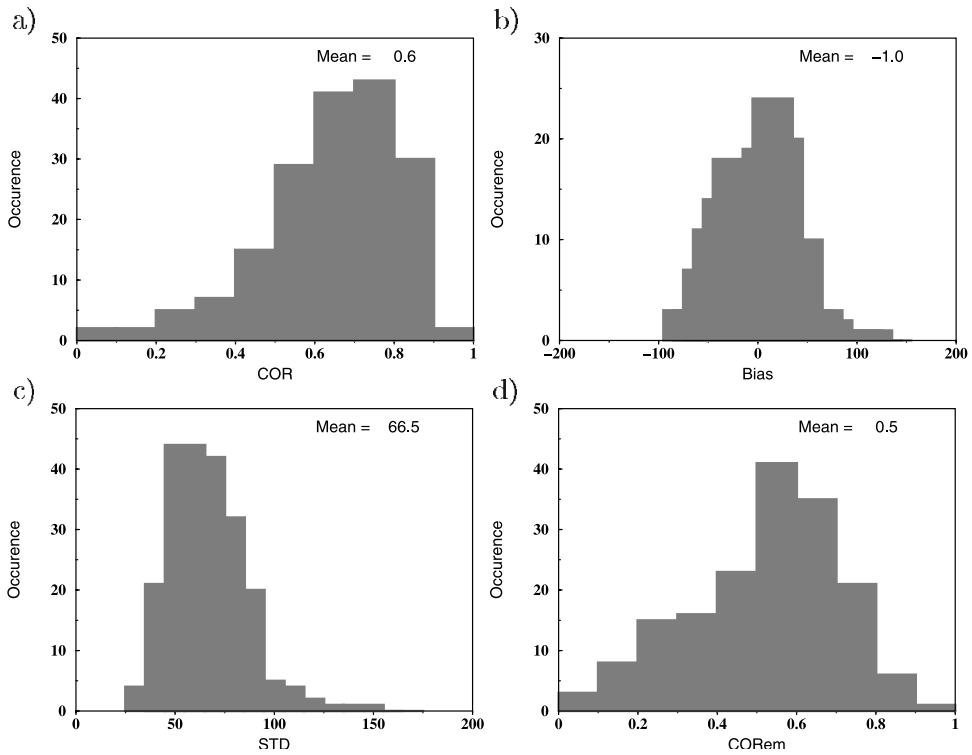

Figure 7. Statistics derived from the daily comparison of NO_2 tropospheric columns simulated by CHIMERE and those measured by SCIAMACHY. Bias and STD are the bias and the standard deviation of the simulation-minus-observation residuals given in percentage relative to the daily mean of SCIAMACHY data, respectively. COR is the correlation coefficient computed between observations and simulations; CORem is the correlation coefficient computed between observations and emissions.

it underestimates them, especially over the marine areas. Note, however, that these very low values are near the SCIAMACHY detection limit.

[57] As shown by Figure 6, the long-range transport of NO_2 is less efficient in summer than in winter as deposition and oxidation take place with increasing radiation. The SCIAMACHY NO_2 tropospheric columns correlate (see Table 2) better with emissions during summer (CORem = 0.74, 0.70 in August) than during winter (CORem = 0.48, 0.14 in December). Thus the high correlation coefficients obtained between SCIAMACHY and CHIMERE NO_2 tropospheric columns in winter (COR = 0.79) and in summer (COR = 0.82) suggest that on a seasonal basis, the spatial distribution of emissions and the horizontal transport of NO_2 are correctly represented by CHIMERE.

5.3. Daily Comparison

[58] Figure 7 shows an overview of the error statistics derived from the daily comparison of NO_2 tropospheric columns simulated by CHIMERE and those measured by SCIAMACHY.

[59] The mean correlation coefficient is 0.6. The lowest correlations often appear for cloudy days and days when NO_2 amounts are small. The mean spatial bias is small (−1%). Seventy-four percent of days show bias between ±40% relative to the daily mean of SCIAMACHY data. However, quite large biases appear for some individual days. Absolute bias values are between $\pm 2.5 \times 10^{15}$ molecules/cm^2. The negative biases are found in spring and summer, while the positive biases are found in winter and autumn. The standard deviation (STD) is large with a mean value of 66.5% relative to the daily mean of SCIAMACHY data.

[60] Figures 8 and 9 show maps of NO_2 SCIAMACHY tropospheric columns and NO_2 CHIMERE tropospheric columns for eight selected days. Figure 10 presents the corresponding scatterplots. The days have been selected when (1) there are enough SCIAMACHY observations (more than 100 data), except for 27 February 2003 which presents an interesting case where the SCIAMACHY data detect a NO_2 plume above the North Sea; (2) the data show high NO_2 tropospheric columns above the sea and the ocean where there are less NO_x emissions but more NO_2 issued from transport; (3) the data show typical situations with high NO_2 tropospheric column values above high NO_x emission areas; (4) SCIAMACHY data cover Netherlands where there are representative surface NO_2 observations; (5) SCIAMACHY data and CHIMERE simulations are very consistent; and (6) SCIAMACHY data and CHIMERE simulations show large differences.

[61] We can notice the high spatial and day-to-day variability of tropospheric NO_2. In general, the CTM agrees very well with SCIAMACHY data on the main spatial patterns of NO_2 which do not always correlate with NO_x emissions patterns (for 64% of the days, correlation coefficients between SCIAMACHY data and the emissions data are lower than 0.6; cf. Figure 7). Large differences appear

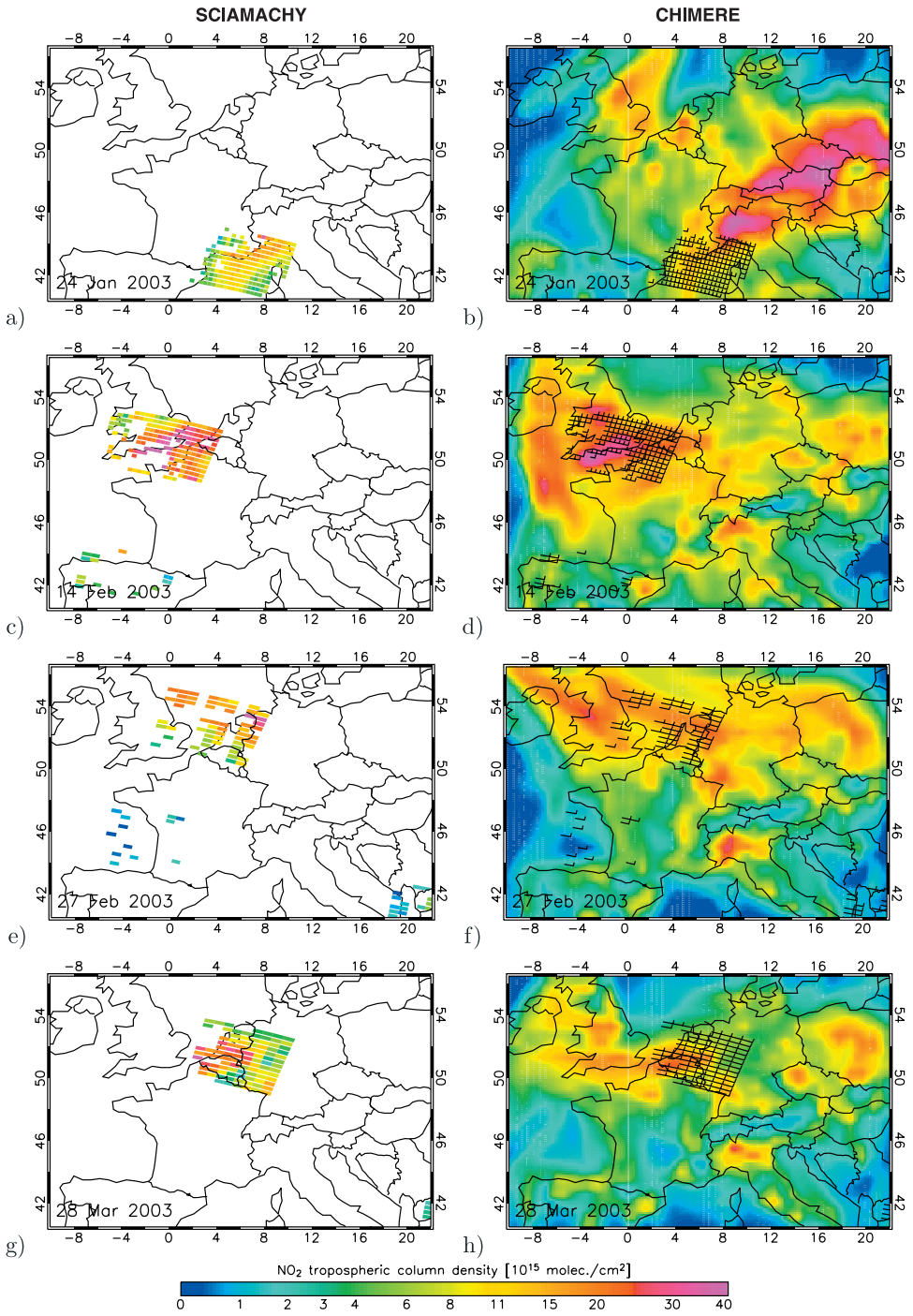

Figure 8. Comparisons between NO_2 SCIAMACHY tropospheric columns (10^{15} molecules/cm^2) on the left and NO_2 CHIMERE tropospheric columns on the right, for (a, b) 24 January 2003, (c, d) 14 February 2003, (e, f) 27 February 2003, (g, h) 28 March 2003, 10h00 UTC. The symbols in the panels on the right indicate the locations of the lower-right corner of the SCIAMACHY observations.

for the highest NO_2 tropospheric columns. High observed NO_2 columns are often underestimated by the CTM.

[62] On 27 February, CHIMERE and SCIAMACHY tropospheric columns agree with a south-north NO_2 gradient in Netherlands. The surface observations and simulations also show a gradient of NO_2 concentrations between the south (high values) and the north (low values) of Netherlands (see Figure 4), but this gradient is reversed compared to that of observed by SCIAMACHY. This suggests that the plume was transported at higher altitude. On this day, CHIMERE overestimates the surface NO_2 concentrations in the north and underestimates them in the south.

[63] On 16 April, CHIMERE is low compared to SCIAMACHY by more than 5×10^{15} molecules/cm^2 over

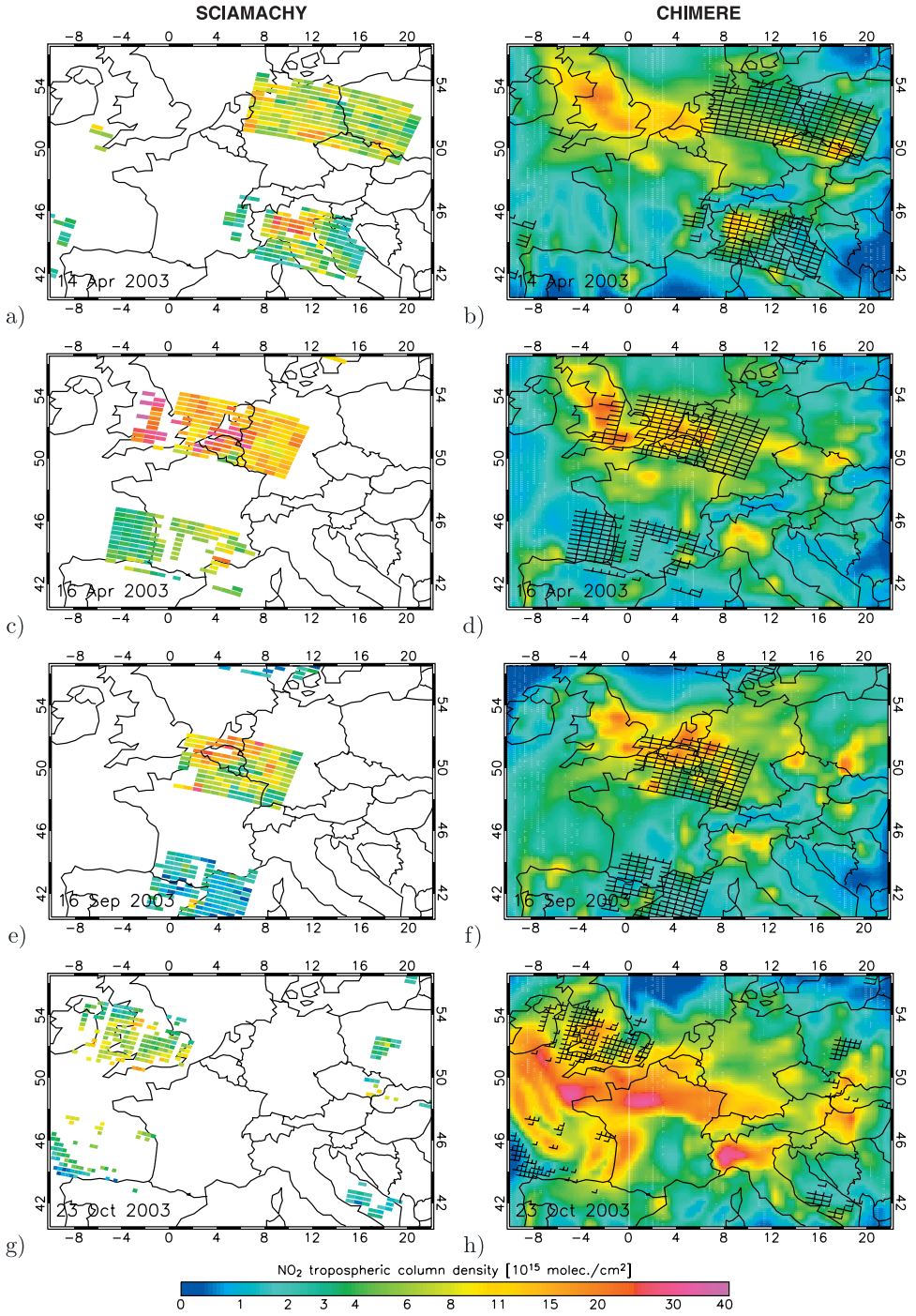

Figure 9. Same with Figure 6 for (a, b) 14 April 2003, (c, d) 16 April 2003, (e, f) 16 September 2003, and (g, h) 23 October 2003. The symbols in the panels on the right indicate the locations of the lower-right corner of the SCIAMACHY observations.

a large part of the observed area. Such differences are also noted at the surface where the CTM underestimates the surface observations of about 5–10 ppb on London, near Paris, and on Netherlands (cf. Section 4). These results suggest that for this day, there is a problem on a large scale; 16 April was characterized by sunny weather conditions. Since such underestimations are rare and concern both the surface and the columns, they cannot be only explained by errors in the emission database and the modeling parameterizations of the vertical mixing and deposition. However, the photochemistry may be disturbed by the presence of Saharan dust as observed by Moderate-Resolution Imaging Spectrometer (MODIS) [*Remer et al.*, 2005] (see gallery on http://rapidfire.sci.gsfc.nasa.gov) and simulated by Navy Aerosol Analysis and Prediction System (NAAPS) Global Aerosol Model (developed by *Christensen* [1997]; see archive on http://www.nrlmry.navy.mil/). As shown by *Martin et al.* [2003], photochemical effects of aerosols generally result in

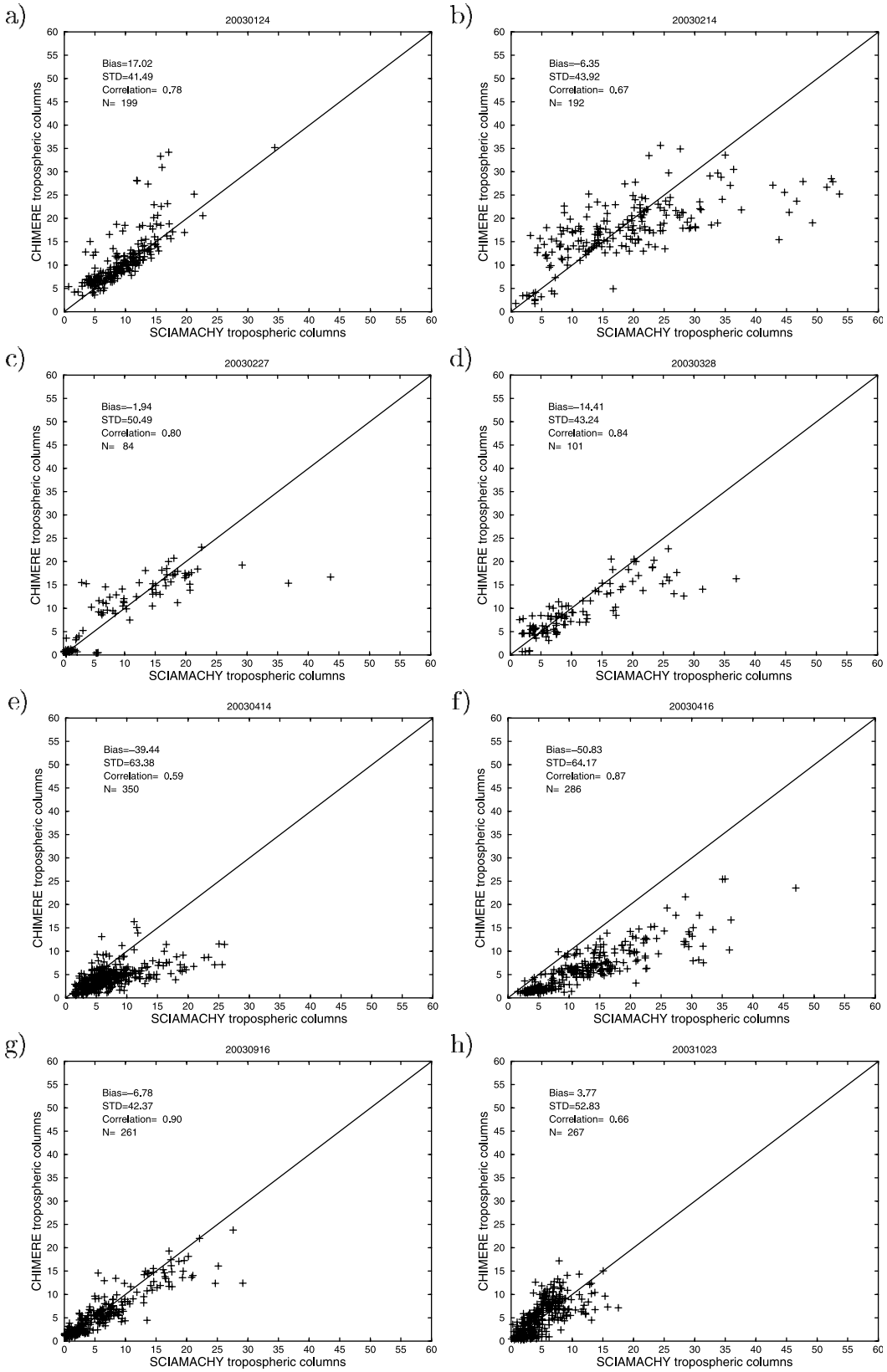

Figure 10. Scatterplots of NO_2 SCIAMACHY tropospheric columns (x axis) versus NO_2 CHIMERE tropospheric columns (y axis). Columns are in 10^{15} molecules/cm^2. Bias and STD are in percent. N is the number of data.

an increase of NO_x because of an OH depletion. The complete analysis of this period will deserve a special paper.

6. Summary and Conclusions

[64] In this paper, we presented (1) a new SCIAMACHY tropospheric NO_2 data set for the year 2003, (2) a comparison between surface NO_2 measurements, NO_2 surface concentrations simulated using a state-of-the-art regional scale air quality model (CHIMERE) and SCIAMACHY NO_2 tropospheric columns, (3) a detailed comparison between this SCIAMACHY data set and NO_2 tropospheric columns simulated by the model. We performed a comparison of the cloud-free satellite observations with collocated model tropospheric columns through the averaging kernel profiles of the satellite retrieval. In this way, we removed the dependency of the comparison on a priori NO_2 profile information used in the retrieval.

[65] From the comparison with the surface sites, we conclude that the CHIMERE model is able to describe NO_2 surface concentrations at rural sites for which measurements are representative of large areas. In the same way, these surface measurements correlate well with the SCIAMACHY NO_2 tropospheric columns. On the contrary, NO_2 concentrations for urban and suburban stations are systematically underestimated by the CTM. This is mainly attributed to the low spatial representativeness of the NO_2 surface measurements in areas with strong gradients of concentrations. One of the conclusions is that the NO_2 surface measurements performed in urban areas cannot be used to validate CTMs or spatial sensors having resolution greater than some kilometers.

[66] Simulated yearly mean total NO_2 tropospheric columns compare very well with the corresponding SCIAMACHY measurements, both spatially and quantitatively (correlation coefficient of 0.87, bias of 5%, RMSE of 45%). Good agreements have been found both in rural and urban areas. The overall seasonality of NO_2 concentrations is similar in both the observations and the simulations, but the amplitude of the seasonal variation is somewhat smaller in SCIAMACHY data than in the model data. The CTM overestimates the SCIAMACHY NO_2 columns during autumn-winter (positive bias of 7–23%) and underestimates them during spring-summer (negative bias of 17–19%). This is consistent with results obtained at the surface. The introduction of a new sink of NO_x induced by the hydrolysis of N_2O_5 on aerosols could reduce the model overestimations in autumn-winter. In order to understand spring-summer underestimations, further investigations are needed. Indeed, spring and summer 2003 were characterized by exceptionally warm conditions and a likely overestimation of the dry deposition [*Vautard et al.*, 2005]. We also show that the CTM tends to systematically underestimate NO_2 tropospheric columns over intense NO_x emission areas, a fact that remains unexplained but could be due to underestimations in the emissions. Such emission underestimations could also contribute to explain the CTM underestimations of surface NO_2 measurements on urban sites. Correlations between NO_2 columns and NO_x emissions are high in summer and low in winter related to seasonal changes in lifetime and transport. High correlation coefficients obtained between model and observed NO_2 tropospheric columns suggest that on a seasonal basis, the spatial distribution of the NO_x emissions, the transport, and the chemistry of NO_2 are quite correctly represented in CHIMERE.

[67] A strong day-to-day variability has been observed in both the SCIAMACHY data and the CHIMERE NO_2 column distributions. The extent of the NO_2 plumes, their location, and the NO_2 tropospheric content are generally similar in observations and simulations, even far from NO_x emission sources. This demonstrates that the model description of horizontal and vertical transport, as well as the lifetime of NO_x, is realistic. It also demonstrates the ability of the satellite to measure a wide range of NO_2 values (spanning 2 orders of magnitude). However, for some days, we found biases between CHIMERE and SCIAMACHY NO_2 tropospheric columns of the order of 2.5×10^{15} molecules/cm^2 (positive in winter and negative in summer) and large standard deviations (STD $\geq$ 50%). For 16 April 2003, we especially noted strong CTM underestimations which could be explained by the presence of Saharan dust over Europe. Taking into account aerosols and their photochemical effect on NO_2 could improve the simulations. We also found that the differences in the NO_2 tropospheric contents do not always agree with differences noted at the surface suggesting that there are sometimes inconsistencies in the vertical distribution of pollutants in CHIMERE.

[68] The simulation-observation differences are due to a combination of model and observation errors. The model errors include errors in the transport, emissions (due to uncertainties in their intensity and their time variabilities), chemistry, boundary conditions, and errors related to the model resolution. The observation errors are due to errors in the cloud and aerosol characterization and surface albedo used for the retrievals. The simulation-observation differences will be investigated in more detail for specific periods in future studies in order to better identify the error sources. The use of more observations (vertical profiles of NO_2 and other satellite observations) will help. Nevertheless, our study suggests that especially the description of NO_x emissions, the chemistry, and the deposition during warm episode deserve special attention. The impact of heterogeneous chemistry (impact of aerosols) will be especially quantified.

[69] To conclude, the fair degree of consistency found between the three independent data sets gives us confidence in both the air quality model results and the SCIAMACHY satellite retrievals. The combination of space and surface observations may impose very strong constraints on air-quality models and could be used to test various model processes, including emission strengths and NO_x lifetimes. In this way the satellite observations of SCIAMACHY and the Ozone Monitoring Instrument aboard EOS-AURA should provide a significant contribution to the assessment of air quality.

[70] **Acknowledgments.** Financial support for the study was provided by the Centre National d'Etude Spatial (CNES), the Marie-Curie Actions, and the ESA/ESRIN DUP-II TEMIS project. The authors would like to thank Martin Schultz from the Max-Planck-Institute for Meteorology in Hamburg for providing MOZART monthly mean fields and Dirk Olivié from Royal Netherlands Meteorological Institute (KNMI) for helpful discussions about convection. The following institutions are also gratefully acknowledged: Météo-France and the European Center for Medium-Range Weather Forecast (ECMWF) for allowing free access to the meteorological database, Agence de l'Environnement et de Maıcirc;trise de l'Energie (ADEME), Department of the Environment, Transport, and the Regions

(DETR), and Landelijk Meetnet Luchtkwaliteit (LML, RIVM) for providing free access to NO_2 surface observations.

References

Aas, W., A.-G. Hjellbrekke, and J. Schaug (2000), Data quality 1998, quality assurance, and field comparisons, EMEP/CCC-Report 6/2000.

Beekmann, M., and C. Derognat (2003), Monte Carlo uncertainty analysis of a regional-scale transport chemistry model constrained by measurements from the Atmospheric Pollution Over the Paris Area (ESQUIF) campaign, *J. Geophys. Res.*, *108*(D17), 8559, doi:10.1029/2003JD003391.

Bessagnet, B., A. Hodzic, R. Vautard, M. Beekmann, S. Cheinet, C. Honor, C. Liousse, and L. Rouil (2004), Aerosol modeling with CHIMERE—Preliminary evaluation at the continental scale, *Atmos. Environ.*, *38*, 2803–2817.

Blond, N., and R. Vautard (2004), Three-dimensional ozone analyses and their use for short-term ozone forecasts, *J. Geophys. Res.*, *109*, D17303, doi:10.1029/2004JD004515.

Blond, N., L. Bel, and R. Vautard (2003), Three-dimensional ozone data analysis with an air quality model over the Paris area, *J. Geophys. Res.*, *108*(D23), 4744, doi:10.1029/2003JD003679.

Boersma, K. F., H. J. Eskes, and E. J. Brinksma (2004), Error analysis for tropospheric NO_2 retrieval from space, *J. Geophys. Res.*, *109*, D04311, doi:10.1029/2003JD003962.

Boersma, K. F., H. J. Eskes, E. W. Meijer, and H. M. Kelder (2005), Estimates of lightning NOx production from GOME satellite observations, *Atmos. Chem. Phys. Disc.*, *5*, 3047–3104.

Bogumil, K., J. Orphal, S. Voigt, H. Bovensmann, O. C. Fleischmann, M. Hartmann, T. Homann, P. Spietz, and J. P. Burrows (1999), Spectra of atmospheric trace gases measured with the SCIAMACHY PFM satellite spectrometer, *Proc. Europ. Sympos. Atm. Meas. Space*, ESA-WPP-161 Vol. II, pp. 443–446.

Bovensmann, H., J. P. Burrows, M. Buchwitz, J. Frerick, S. Noël, V. V. Rozanov, K. V. Chance, and A. P. H. Goede (1999), SCIAMACHY: Mission objectives and measurement modes, *J. Atmos. Sci.*, *56*, 127–150.

Builtjes, P. (1992), The LOTOS—Long Term Ozone Simulation—Project; summary report, TNO-IMW-report R 92/240, Delft, Netherlands.

Burrows, J. P., et al. (1999), The global ozone Monitoring Experiment (GOME): Mission concept and first scientific results, *J. Atmos. Sci.*, *56*, 151–175.

Cardelino, C., M. Chang, J. St. John, B. Murphey, J. Cordle, R. Ballagas, L. Patterson, K. Powell, J. Stogner, and S. Zimmer-Dauphinee (2001), Ozone predictions in Atlanta, Georgia: Analysis of the 1999 ozone season, *J. Air Waste Manage. Assoc.*, *51*, 1227–1236.

Chance, K. (1998), Analysis of BrO measurements from the Global Ozone Monitoring Experiment, *Geophys. Res. Lett.*, *25*, 3335–3338.

Chance, K., P. I. Palmer, R. J. D. Spurr, R. V. Martin, T. P. Kurosu, and D. J. Jacob (2000), Satellite observations of formaldehyde over North America from GOME, *Geophys. Res. Lett.*, *27*, 3461–3464.

Christensen, J. H. (1997), The Danish Eulerian hemispheric model—A three-dimensional air pollution model used for the Arctic, *Atmos. Environ.*, *31*, 4169–4191.

Chu, D. A., Y. J. Kaufman, G. Zibordi, J. D. Chern, J. Mao, C. Li, and B. N. Holben (2003), Global Monitoring of Air Pollution over land from EOS-Terra MODIS, *J. Geophys. Res.*, *108*(D21), 4661, doi:10.1029/2002JD003179.

Colvile, R. N., E. J. Hutchinson, J. S. Mindell, and R. F. Warren (2001), The transport sector as a source of air pollution, *Atmos. Environ.*, *35*(9), 1537–1565.

Cuvelier, C., et al. (2007), CityDelta: A model intercomparison study to explore the impact of emission reductions in European cities in 2010, *Atmos. Environ.*, *41*(1), 189–207.

de Haan, J. F., P. B. Bosma, and J. W. Hovenier (1987), The adding method for multiple scattering calculations of polarised light, *Astron. Astrophys.*, *183*, 371–391.

Dentener, F. J., and P. J. Crutzen (1993), Reaction of N2O5 on tropospheric aerosols: Impact on the global distributions of NOx, O3, and OH, *J. Geophys. Res.*, *98*(D4), 7149–7163.

Dentener, F., M. van Weele, M. Krol, S. Houweling, and P. van Velthoven (2002), Trends and inter-annual variability of methane emissions derived from 1979–1993 global CTM simulations, *Atmos. Chem. Phys. Discuss.*, *2*, 249–287.

Derognat, C., M. Beekmann, M. Baeumle, D. Martin, and H. Schmidt (2003), Effect of biogenic volatile organic compound emissions on tropospheric chemistry during the Atmospheric Pollution Over the Paris Area (ESQUIF) campaign in the Ile-de-France region, *J. Geophys. Res.*, *108*(D17), 8560, doi:10.1029/2001JD001421.

Eisinger, M., and J. P. Burrows (1998), Tropospheric sulfur dioxide observed by the ERS-2 GOME instrument, *Geophys. Res. Lett.*, *25*, 4177–4180.

Elbern, H., and H. Schmidt (2001), Ozone episode analysis by four-dimensional variational chemistry data assimilation, *J. Geophys. Res.*, *106*, 3569–3590.

Emmons, L. K., et al. (2004), Validation of measurements of pollution in the troposphere (MOPITT) CO retrievals with aircraft in situ profiles, *J. Geophys. Res.*, *109*(D3), D03309, doi:10.1029/2003JD004101.

Eskes, H. J., and K. F. Boersma (2003), Averaging kernels for DOAS total-column satellite retrievals, *Atmos. Chem. Phys.*, *3*, 1285–1291.

ESQUIF (2001), Etude et Simulation de la qualité de l'air en Île-de-France, rapport final, Institut Pierre Simon Laplace.

Generation of European Emission Data for Episodes (GENEMIS) project (1994), EUROTRAC annual report 1993, part 5, EUROTRAC international scientific secretariat, Garmisch-Partenkirchen, Germany.

Gerboles, M., F. Lagler, D. Rembges, and C. Brun (2003), Assessment of uncertainty of NO_2 measurements by the chemiluminescence method and discussion of the quality objective of the NO_2 European Directive, *J. Environ. Monit.*, *5*(4), 529–540.

Greenblatt, G. D., J. J. Orlando, J. B. Burkholder, and A. R. Ravishankara (1990), Absorption measurements of oxygen between 330 and 1140 nm, *J. Geophys. Res.*, *95*, 18,577–18,582.

Hanna, S. R., J. C. Chang, and M. E. Fernau (1998), Monte Carlo estimates of uncertainties in predictions by a photochemical grid model (UAM-IV) due to uncertainties in input variables, *Atmos. Environ.*, *32*, 3619–3628.

Hass, H., P. J. H. Builtjes, D. Simpson, and R. Stern (1997), Comparison of model results obtained with several European regional air quality models, *Atmos. Environ.*, *31*(19), 3259–3279.

Heland, J., H. Schlager, A. Richter, and J. P. Burrows (2002), First comparison of tropospheric NO_2 column densities retrieved from GOME measurements and in situ aircraft profile measurements, *Geophys. Res. Lett.*, *29*(20), 1983, doi:10.1029/2002GL015528.

Herman, J. R., and E. A. Celarier (1997), Earth surface reflectivity climatology at 340 nm to 380 nm from TOMS data, *J. Geophys. Res.*, *102*, 28,003–28,011.

Hodzic, A., R. Vautard, B. Bessagnet, M. Lattuati, and F. Moreto (2005), Long-term urban aerosol simulation versus routine particulate matter observations, *Atmos. Environ.*, *39*, 5851–5864.

Horowitz, L. W., et al. (2003), A global simulation of tropospheric ozone and related tracers: Description and evaluation of MOZART, version 2, *J. Geophys. Res.*, *108*(D24), 4784, doi:10.1029/2002JD002853.

Koelemeijer, R. B. A., P. Stammes, J. W. Hovenier, and J. F. de Haan (2001), A fast method for retrieval of cloud parameters using oxygen A-band measurements from GOME, *J. Geophys. Res.*, *106*, 3475–3490.

Koelemeijer, R. B. A., J. F. de Haan, and P. Stammes (2003), A database of spectral surface reflectivity in the range 335–772 nm derived from 5.5 years of GOME observations, *J. Geophys. Res.*, *108*(D2), 4070, doi:10.1029/2002JD002429.

Konovalov, I. B., M. Beekmann, R. Vautard, J. P. Burrows, A. Richter, and H. N. N. Elansky (2004), Comparison and evaluation of modelled and GOME measurement derived tropospheric NO_2 columns over Western and Eastern Europe, *Atmos. Chem. Phys. Disc.*, *4*, 6503–6558.

Kuhlwein, J., and R. Friedrich (2000), Uncertainties of modeling emissions from road transport, *Atmos. Environ.*, *34*, 4603–4610.

Lambert, J.-C., et al. (2004), Geophysical Validation of SCIAMACHY NO_2 Vertical Columns: Overview of Early 2004, Proceedings of the Second Workshop on the Atmospheric Chemistry Validation of ENVISAT (ACVE-2), 3–7 May 2004, ESA-ESRIN, Frascati, Italy (ESA SP-562).

Lattuati, M. (1997), Contribution à l'étude du bilan de l'ozone troposphérique à l'interface de l'Europe et de l'Atlantique Nord: Modélisation lagrangienne et mesures en altitude, PhD thesis, Université Paris 6, Paris.

Lauer, A., M. Dameris, A. Richter, and J. P. Burrows (2002), Tropospheric NO_2 columns: A comparison between model and retrieved data from GOME measurements, *Atmos. Chem. Phys.*, *2*, 67–78.

Leue, C., M. Wenig, T. Wagner, O. Klimm, U. Platt, and B. Jähne (2001), Quantitative analysis of NOx emissions from Global Ozone Monitoring Experiment satellite image sequences, *J. Geophys. Res.*, *106*, 5493–5505.

Lu, R., R. P. Turco, and M. Z. Jacobson (1997a), An integrated air pollution modeling system for urban and regional scale: 1: Model formulation and numerics, *J. Geophys. Res.*, *102*, 6063–6079.

Lu, R., R. P. Turco, and M. Z. Jacobson (1997b), An integrated air pollution modeling system for urban and regional scale: 2: Evaluation of model performance using SCAQS data, *J. Geophys. Res.*, *102*, 6081–6098.

McNair, L. A., R. A. Harley, and A. G. Russell (1996), Spatial inhomogeneity in pollutant concentrations and implications for air quality model evaluation, *Atmos. Environ.*, *30*(24), 4291–4301.

Madronich, S., and S. Flocke (1998), The role of solar radiation in atmospheric chemistry, in *Handbook of Environmental Chemistry*, edited by P. Boule, pp. 1–26, Springer, New York.

Martin, R. V., et al. (2002), An improved retrieval of tropospheric nitrogen dioxide from GOME, *J. Geophys. Res.*, *107*(D20), 4437, doi:10.1029/2001JD001027.

Martin, R. V., D. J. Jacob, R. M. Yantosca, M. Chin, and P. Ginoux (2003), Global and regional decreases in tropospheric oxidants from photoche-

mical effects of aerosols, *J. Geophys. Res.*, *108*(D3), 4097, doi:10.1029/2002JD002622.
Martin, R. V., D. D. Parrish, T. B. Ryerson, D. K. Nicks Jr., K. Chance, T. P. Kurosu, A. Fried, B. P. Wert, D. J. Jacob, and E. D. Sturges (2004), Evaluation of GOME satellite measurements of tropospheric NO_2 and HCHO using regional data from aircraft campaigns in the southeastern United States, *J. Geophys. Res.*, *109*, D24307, doi:10.1029/2004JD004869.
Matthews, R. D., R. F. Sawyer, and R. W. Schefer (1977), Interferences in chemiluminescent measurement of NO and NO_2 emissions from combustion systems, *Environ. Sci. Technol.*, *11*, 1092–1096.
Mentel, Th. F., D. Bleilebens, and A. Wahner (1996), A study of nighttime nitrogen oxide oxidation in a large reaction chamber—The fate of NO_2, N_2O_5, HNO_3, and O_3 at different humidities, *Atmos. Environ.*, *30*, 4007–4020.
Menut, L., et al. (2000), Measurements and modeling of atmospheric pollution over the Paris area: An overview of the ESQUIF project, *Ann. Geophys.*, *18*, 1467–1481.
Menut, L. (2003), Adjoint modeling for atmospheric pollution process sensitivity at regional scale, *J. Geophys. Res.*, *108*(D17), 8562, doi:10.1029/2002JD002549.
Moussiopoulos, N., P. Sahm, K. Karatzas, S. Papalexiou, and A. Karagiannidis (1997), Assessing the impact of the new Athens airport to urban air quality with contemporary air pollution models, *Atmos. Environ.*, *31*, 1497–1511.
Olivié, D. J. L., P. F. J. van Velthoven, A. C. M. Beljaars, and H. M. Kelder (2004), Comparison between archived and off-line diagnosed convective mass fluxes in the chemistry transport model TM3, *J. Geophys. Res.*, *109*, D11303, doi:10.1029/2003JD004036.
Ordóñez, C., A. Richter, M. Steinbacher, C. Zellweger, H. Nüß, J. P. Burrows, and A. S. H. Prévôt (2006), Comparison of 7 years of satellite-borne and ground-based tropospheric NO_2 measurements around Milan, Italy, *J. Geophys. Res.*, *111*, D05310, doi:10.1029/2005JD006305.
Perl, A., J. Patterson, and M. Perez (1997), Pricing aircraft emissions at Lyon-Satolas Airport, *Transp. Res. D*, *2*(2), 89–105.
Petritoli, A., P. Bonasoni, G. Giovanelli, F. Ravegnani, I. Kostadinov, D. Bortoli, A. Weiss, D. Schaub, A. Richter, and F. Fortezza (2004), First comparison between ground-based and satellite-borne measurements of tropospheric nitrogen dioxide in the Po basin, *J. Geophys. Res.*, *109*, D15307, doi:10.1029/2004JD004547.
Platt, U. (1994), Differential optical absorption spectroscopy (DOAS), *Chem. Anal. Series*, *127*, 27–83.
Remer, L. A., et al. (2005), The MODIS aerosol algorithm, products and validation, *J. Atmos. Sci.*, *62*, 947–973.
Richter, A., and J. P. Burrows (2002), Tropospheric NO_2 from GOME measurements, *Adv. Space Res.*, *29*, 1673–1683.
Rickman, E. E., Jr., and R. S. Wright (1986), Interference of nitrogenous compounds on chemiluminescent measurement of nitrogen dioxide, Research Triangle Institute (Report No. RTI/3180/24-01F), Research Triangle Park, N. C.
Rothman, L. S. (1992), The HITRAN data base, *J. Quant. Spectrosc. Radiat. Transfer*, *48*, 5–6.
Savage, N. H., K. S. Law, J. A. Pyle, A. Richter, H. Nuess, and J. P. Burrows (2004), Using GOME NO_2 satellite data to examine regional differences in TOMCAT model performance, *Atmos. Chem. Phys.*, *4*, 1895–1912.
Schaub, D., K. F. Boersma, J. W. Kaiser, A. K. Weiss, D. Folini, H. J. Eskes, and B. Buchmann (2006), Comparison of GOME tropospheric NO2 columns with NO2 profiles deduced from ground-based in situ measurement, *Atmos. Chem. Phys.*, *6*, 3211–3229.
Schmidt, H., C. Derognat, R. Vautard, and M. Beekmann (2001), A comparison of simulated and observed ozone mixing ratios for the summer of 1998 in western Europe, *Atmos. Environ.*, *35*, 6277–6297.
Silibello, C., G. Calori, G. Brusasca, G. Catenacci, and G. Finzi (1998), Application of a photochemical grid model to Milan metropolitan area, *Atmos. Environ.*, *32*(11), 2025–2038.
Simpson, D. (1992), Long period modeling of photochemical oxidants in Europe, calculations for July 1985, *Atmos. Environ.*, *26*, 1609–1634.
Simpson, D., H. Fagerli, J. E. Jonson, S. Tsyro, P. Wind, and J.-P. Tuovinen (2003), Transboundary acidification, eutrophication and ground level ozone in Europe, Part I, Unified EMEP model description, EMEP status report 1/2003, ISSN 0806-4520.
Stammes, P. (2001), Spectral radiance modelling in the UV-visible range, in *IRS 2000: Current Problems in Atmospheric Radiation*, edited by W. L. Smith and Y. M. Timofeyev, pp. 385–388.
Stammes, P., J. F. de Haan, and J. W. Hovenier (1989), The polarized internal radiation field of a planetary atmosphere, *Astron. Astrophys.*, *225*, 239–259.
Stohl, A., E. Williams, G. Wotawa, and H. Kromp-Kolb (1996), A European inventory of soil nitric oxide emissions and the effect of these emissions on the photochemical formation of ozone, *Atmos. Environ.*, *30*, 3741–3755.
Suutari, R., M. Amann, J. Cofala, Z. Klimont, M. Posch, and W. Schopp (2001), From Economic Activities to Ecosystem Protection in Europe. An Uncertainty Analysis of Two Scenarios of the RAINS Integrated Assessment Model, EMEP CIAM/CCE Report 1/2001, International Institute for Applied Systems Analysis, Laxenburg, Austria.
Tiedtke, M. (1989), A comprehensive mass flux scheme for cumulus parameterization in large-scale models, *Mon. Weather Rev.*, *117*, 1779–1800.
Tilmes, S., and J. Zimmermann (1998), Investigation on the spatial scales of the variability in measured near-ground ozone mixing ratios, *Geophys. Res. Lett.*, *25*, 3827–3830.
Tilmes, S., et al. (2002), Comparison of five Eulerian ozone prediction systems for summer 1999 using the German monitoring data, *J. Atmos. Chem.*, *42*, 91–121.
Valks, P. J. M., R. B. A. Koelemeijer, M. Van Weele, P. Van Velthoven, J. P. F. Fortuin, and H. Kelder (2003), Variability in tropical tropospheric ozone: Analysis with Global Ozone Monitoring Experiment observations and a global model, *J. Geophys. Res.*, *108*(D11), 4328, doi:10.1029/2002JD002894.
Vautard, R., M. Beekmann, J. Roux, and D. Gombert (2001), Validation of a hybrid forecasting system for the ozone concentrations over the Paris area, *Atmos. Environ.*, *35*, 2449–2461.
Vautard, R., et al. (2003a), Paris emission inventory diagnostics from ESQUIF airborne measurements and a chemistry transport model, *J. Geophys. Res.*, *108*(D17), 8564, doi:10.1029/2002JD002797.
Vautard, R., et al. (2003b), A synthesis of the air pollution over the Paris region (ESQUIF) field campaign, *J. Geophys. Res.*, *108*(D17), 8558, doi:10.1029/2003JD003380.
Vautard, R., C. Honor, M. Beekmann, and L. Rouil (2005), Simulation of ozone during the August 2003 heat wave and emission control scenarios, *J. Atmos. Environ.*, *39*, 2957–2967.
van der A, R. J., D. H. M. U. Peters, H. Eskes, K. F. Boersma, M. Van Roozendael, I. De Smedt, and H. M. Kelder (2006), Detection of the trend and seasonal variation in tropospheric NO2 over China, *J. Geophys. Res.*, *111*, D12317, doi:10.1029/2005JD006594.
van de Velde, R., W. Faber, V. Katwijk, H. J. Scholten, T. J. M. Thewessen, M. Verspuy, and M. Zevenbergen (1994), The preparation of a European land-use database, RIVM Report 712401001, Bilthoven, Netherlands.
Velders, G. J. M., C. Granier, R. W. Portmann, K. Pfeilsticker, M. Wenig, T. Wagner, U. Platt, A. Richter, and J. P. Burrows (2001), Global tropospheric NO_2 column distributions: Comparing three-dimensional model calculations with GOME measurements, *J. Geophys. Res.*, *106*(D12), 12,643–12,660.
Verwer, J. G. (1994), Gauss-Seidel iteration for stiff ODEs from chemical kinetics, *SIAM J. Sci. Comput.*, *15*, 1243–1250.
Vestreng, V., M. Adams, and J. Goodwin (2004), Inventory Review 2004, Emission Data reported to CLRTAP and under the NEC Directive, EMEP/EEA Joint Review Report, EMEP/MSC-W Note 1/2004. ISSN 0804-2446.
Vountas, M., V. V. Rozanov, and J. P. Burrows (1998), Ring effect: Impact of rotational Raman scattering on radiative transfer in Earth's atmosphere, *J. Quant. Spectrosc. Radiat. Transfer*, *60*, 943.
Wang, J., and S. A. Christopher (2003), Intercomparison between satellite-derived aerosol optical thickness and PM2.5 mass: Implications for air quality studies, *Geophys. Res. Lett.*, *30*(21), 2095, doi:10.1029/2003GL018174.
Winer, A. M., J. W. Peters, J. P. Smith, and J. N. Pitts Jr. (1974), Response of commercial chemiluminescent NO-NO_2 analyzers to other nitrogen-containing compounds, *Environ. Sci. Technol.*, *8*, 1118–1121.
Zlatev, Z., J. Christensen, and O. Hov (1992), An Eulerian air pollution model for Europe with nonlinear chemistry, *J. Atmos. Chem.*, *15*, 1–37.

G. Bergametti, Laboratoire Interuniversitaire des Systèmes Atmosphériques, Universités Paris 7 et 12, UMR CNRS 7583, 61, Av. du Général de Gaulle, F-94010, Créteil, France. (bergametti@lisa.univ-paris12.fr)

N. Blond, Laboratoire Image et Ville, Université Louis Pasteur, UMR CNRS 7011, 3, rue de l'Argonne, F-67000, Strasbourg, France. (nadege.blond@lorraine.u-strasbg.fr)

K. F. Boersma, H. J. Eskes, and R. van der A, Atmospheric Composition Climate Research, Royal Netherlands Meteorological Institute, De Bilt, Netherlands. (boersma@knmi.nl; eskes@knmi.nl; avander@knmi.nl)

I. De Smedt and M. Van Roozendael, Belgian Institute for Space Aeronomy (IASB), Ringlaan-3-Avenue Circulaire, B-1180, Brussels, Belgium. (isabelle.desmedt@bira-iasb.oma.be; michel.vanroozendael@bira-iasb.oma.be)

R. Vautard, Laboratoire de Météorologie Dynamique, UMR CNRS 8539, École Polytechnique, F-91128, Palaiseau, France. (vautard@lmd.polytechnique.fr)